Supplemental Appendix for:

Additionality and Asymmetric Information in Environmental Markets: Evidence from Conservation Auctions

Karl M. Aspelund and Anna Russo

A Supplemental Material: Theoretical Framework

$\theta_i = (c_i, a_{i0})$ can be defined in the context of the following model. First, define π as the net payoffs to a landowner from cropping a field. $\pi > 0$ implies expected revenues from harvested crops at the point of planting exceed input costs, whereas $\pi < 0$ implies the opposite. When a landowner chooses $x_i = 1$, she makes a long-term (binding, ten-year) promise to conserve the fields on her land. At the point of contracting, each landowner faces stochastic and heterogeneous net payoffs to cropping each of her fields over the contract period. Therefore, define $h_i(\pi)$ as the probability density function describing landowner i's net payoffs from cropping across fields over the contract period. Finally, define η_i as a landowner's hassle cost type.

When unconstrained by the contract, landowners crop their land when it is profitable to do so. When constrained by the contract, landowners cannot crop — they give up the option — and may incur some hassle cost. Each landowner's type $\theta_i = (c_i, a_{i0})$ can therefore be written as:[49]

$$c_i = \int_0^\infty \pi h_i(\pi)\, d\pi + \eta_i \tag{19}$$

$$a_{i0} = \int_{-\infty}^0 h_i(\pi)\, d\pi. \tag{20}$$

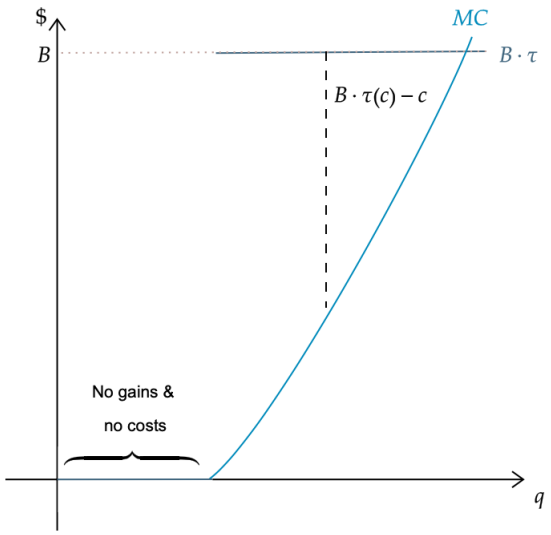
Equations (19) and (20) clarify why the graphs in Section I. may feature upwards-sloping contract value curves ($\tau'(c) > 0$): both c_i and a_{i0} depend on $h_i(\pi)$. They also clarify why *both* f_C and $\tau(c)$ must be estimated empirically. $\tau(c)$ is generally ambiguous, given f_C.

Special Case The microfoundation is useful to explore an important, one-dimensional special case with a single field without uncertainty or hassle costs. In this special case, $h_i(\pi)$ has mass only at a single point, π_i, and $\eta_i = 0$ for all i. Therefore, $c_i = \mathbb{1}\{\pi_i > 0\} \cdot \pi_i$ and $a_{i0} = \mathbb{1}\{\pi_i \leq 0\}$.

Appendix Figure A.1 illustrates this case in the graphical analysis of Section I. There is a mass at zero, where $\pi_i < 0$, so $c_i = 0$ and $\tau(0) = 0$: these are landowners for whom accepting the contract *both* imposes no costs ($c_i = 0$) and has no impact ($\tau(0) = 0$). For any $c > 0$, $\tau(c) = 1$.

[49] Note that here, a_{i0} is defined ex-ante at the time of contracting, corresponding to the definition of c_i, whereas in our empirical tests we observe the realization of the action a_{i0}. However, recall that our welfare criterion in the graphical analysis of Section I. and our estimation and counterfactual analysis is defined as a function of the conditional expectation function $\tau(c) = \mathbb{E}[1 - a_{i0} \mid c = c_i]$. We therefore take expectations across realizations among landowners with the same c_i, making the assumption that landowners' expectations about the payoffs to cropping are correct on average, across years and among landowners with the same c_i.

Figure A.1: Graphical Analysis: One-Dimensional Special Case



Notes: Figure describes a market characterized by a marginal cost ($MC = F_C^{-1}(q)$) and contract value ($B \cdot \tau$) curve for a one-dimensional case in which $\tau(0) = 0$ and $\tau(c) = 1$ for all $c > 0$. The horizontal axis is the share of the population ordered by costs c_i. B denotes the social benefits of $a_{i1} = 1$. $B \cdot \tau$ denotes the incremental social benefits of contracting, relative to no contract, at each quantile of landowner costs c_i. The vertical distance between the $B \cdot \tau$ and MC curves represents the social surplus from contracting, $B \cdot \tau(c) - c$. In this special case, social surplus is not monotonically decreasing in landowner cost. Therefore, while the efficient allocation can be implemented by $p^* = B$, in the presence of a binding quantity constraint, the efficient allocation cannot be implemented.

Figure A.1 illustrate three important points in this special case. First, setting prices at $p^* = B$, the social value of the conservation action (Pigouvian pricing), implements the efficient allocation. Second, $B \cdot \tau(c) - c$ is *not* monotonically decreasing. Given a binding quantity constraint, an efficient allocation subject to that constraint may therefore *not* be implementable. Finally, in Figure A.1, in contrast to the general model described above, knowledge of B and f_C alone are sufficient to evaluate social welfare.

Importantly, distinguishing between this special case and the more general model presented above is possible with a design that estimates additionality, $\tau(c)$, at a given quantile, or among *marginal* landowners. This is because in Figure A.1, $\tau(c)$ can only take values of zero or one. In Section III., we leverage a regression discontinuity design to estimate additionality among marginal landowners and reject this special case.

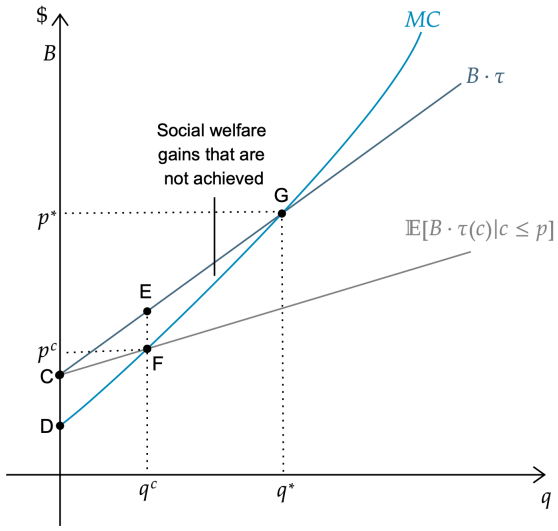
Extension: Competitive Markets We can extend the framework of Section I. to study settings where contracts are traded in competitive markets to capture a stylized model of a voluntary offset market. In a competitive market, adverse selection can prevent the competitive equilibrium price from implementing an efficient allocation, even when it is implementable with the price that solves equation (4) (Akerlof, 1970).

We explore this possibility by making the important simplifying assumption that buyers in this market also value the benefits of land retirement at their social benefits, B, and define a competitive

market price p^c by the equilibrium condition: $p^c = \mathbb{E}\left[B \cdot \tau\left(c_i\right) \mid c_i \leq p^c\right]$. The key distinction is that in this stylized competitive market, the equilibrium price is determined by price-taking buyers taking expectations over the additionality of *all* market participants, not only those contracting at the margin.

Figure A.2 illustrates by adding the curve defined by $\mathbb{E}\left[B \cdot \tau\left(c_i\right) \mid c_i \leq p\right]$ to the population of landowners presented in Figure 1a.[50] Its intersection with the marginal cost curve defines the competitive market equilibrium, which differs from the socially-optimal price. In the presence of adverse selection, trade in this stylized competitive market will be limited and efficient contracting, with social welfare gains represented in triangle EFG, will not occur.

Figure A.2: Graphical Analysis: Competitive Markets



Notes: Figure describes a market characterized by a marginal cost ($MC = F_C^{-1}(q)$) and a contract value ($B \cdot \tau$) curve. The horizontal axis is the share of the population ordered by costs c_i. B denotes the social benefits of $a_{i1} = 1$. $B \cdot \tau$ denotes the incremental social benefits of contracting, relative to no contract, at each quantile of landowner costs. The vertical distance between the $B \cdot \tau$ and MC curves represents the social surplus from contracting. Upwards-sloping $B \cdot \tau$ curves illustrate markets with adverse selection. The figure also includes a curve defining the average contract value of all landowners selecting into the market at any given price p, $\mathbb{E}\left[B \cdot \tau\left(c\right) \mid c \leq p\right]$. This defines the value of a contract to a price-taking buyer in a stylized competitive market. The intersection of the MC and average contract value curves define a competitive market equilibrium price p^c. Adverse selection limits trade, with social welfare gains in triangle EFG that are not achieved.

B Institutional Appendix: The CRP Mechanism

The scoring rule depends on characteristics of the land, the conservation action defined in the contract, and the dollar component of the bid (the bid rental rate). We describe the details associated with each of these components below. The details of the scoring rule are published each year in EBI Factsheets.[51]

Land characteristics The characteristics that influence the scoring rule include:

[50] This curve is defined as $\frac{1}{q}\int_0^q B \cdot \tau\left(F_C^{-1}\left(\tilde{q}\right)\right) d\tilde{q}$.

[51] See an EBI Factsheet for an example.

- **Whether a bidder is in a Wildlife Priority Zone (WPZ)**, defined high priority wildlife geographic areas. 30 points.
- **Whether a bidder is in a Water Quality Zone (WQZ)**, areas with high value to improving ground or surface water quality. 30 points.
- **Groundwater quality**: an evaluation of the predominant soils, potential leaching of pesticides and nutrients into groundwater, and the impact to people who rely on groundwater as a primary source of drinking water. Continuous score: 0 to 25 points.
- **Surface water quality**: an evaluation of the amount of sediment (and associated nutrients) that may be delivered into streams and other water courses. Continuous score: 0 to 45 points.
- **Erosion potential**: Continuous score of 0 to 100 points depending on the Erodibility Index.
- **Air quality**: an evaluation of the air quality improvements by reducing airborne dust and particulate caused by wind erosion from cropland. Continuous score of 0 to 30 points depending on wind speed, wind direction, and the duration of wind events and soil erodibility.
- **Whether a bidder is in an Air Quality Zone (AQZ)**. 5 points.

These characteristics depend on a bidder's location and not their bid, i.e. they determine bidder asymmetry in the scoring rule. These characteristics are known for every agricultural field in the US.

Heterogeneous contracts defined by conservation actions Conservation actions can be grouped into two categories: a primary cover, described in Table B.1, which covers the total area offered into the CRP, and an (optional) additional upgrade action, described in Table B.2, which can be offered in addition to the primary cover on a smaller area. In total, there are 36 possible contracts: 12 primary covers interacted with three upgrade cover options (including no upgrade).

Table B.1: Contract Action Choices: Primary Covers

Short name	Description
Grasses 1	Permanent introduced grasses and legumes (CP1): Existing stand of one to three species or planting new stand of two to three species of an introduced grass species.
Grasses 2	Permanent introduced grasses and legumes (CP1): Existing stand or planted mixture (minimum of four species) of at least 3 introduced grasses and at least one forb or legume species best suited for wildlife in the area.
Grasses 3	Permanent native grasses and legumes (CP2): Existing stand (minimum of one to three species) or planting mixed stand (minimum of three species) of at least two native grass species at least one forb or legume species beneficial to wildlife.
Grasses 4	Permanent native grasses and legumes (CP2): Existing stand or planting mixed stand (minimum of five species) of at least 3 native grasses and at least one shrub, forb, or legume species best suited for wildlife in the area.
Trees 1	Tree planting (softwoods) (CP3): Southern pines, northern conifers, or western pines – solid stand of pines/conifers/softwoods (existing, according to state developed standards, or planted at more than 550 (southern pines), 850 (northern conifers), or 650 (western pines) trees per acre).
Trees 2	Tree planting (softwoods) (CP3): Southern pines, northern conifers, or western pines – pines/conifers/softwoods existing or planted at a rate of 500-550 (southern pines), 750-850 (northern conifers), or 550-650 (western pines) per acre depending on the site index (state-developed standards) with 10-20% openings managed to a CP4D wildlife cover.
Trees 3	Hardwood tree planting (CP3A): Existing or planting solid stand of nonmast producing hardwood species.
Trees 4	Hardwood tree planting (CP3A): Existing or planting solid stand of single hard mast producing species.
Trees 5	Hardwood tree planting (CP3A): Existing or planting mixed stand (three or more species) or hardwood best suited for wildlife in the area or existing or planting stand of longleaf pine or atlantic white cedar – planted at rates appropriate for the site index.
Habitat 1	Permanent wildlife habitat, noneasement (CP4D): Existing stand or planting mixed stand (minimum of four species) of either grasses, trees, shrubs, forbs, or legumes planted in mixes, blocks, or strips best suited for various wildlife species in the area. A wildlife conservation plan must be developed with the participant.
Habitat 2	Permanent wildlife habitat, noneasement (CP4D): Existing stand or planting mixed stand (minimum of five species) or either predominantly native species including grasses, forbs, legumes, shrubs, or trees planted in mixes, blocks, or strips best suited to providing wildlife habitat. Only native grasses are authorized. A wildlife conservation plan must be developed with the participant.
Habitat 3	Rare and declining habitat restoration (CP25): Existing stand or seeding or planting will be best suited for wildlife in the area. Plant species selections will be based upon Ecological Site Description data.

Notes: Table describes the menu of primary cover actions.

Table B.2: Contract Action Choices: Upgrades

Short name	Description
No upgrade	Primary cover only
Wildlife food plot	Wildlife food plots are small plantings in a larger area
Pollinator habitat	Existing stand or planting (minimum of .5 acres) of a diverse mix of multiple species suited for pollinators

Notes: Table describes the menu of upgrade actions.

We obtain the points associated with each of the contract options, defined by the actions in Tables B.1 and B.2 from the EBI Fact Sheets. The point values assigned to the different contracts can vary across bidders based on whether or not a bidder is in a Wildlife Priority Zone (WPZ).

Bid rental rate The scoring rule is non-linear in r_i. The existence of bid caps make some choices infeasible if $r_i > \overline{r}_i$, where $\overline{r}_i$ denotes the landowner specific bid cap. The scoring rule also includes non-linearities based on the amount a bidder bids below the bid cap with kinks at 10% and 15% below the bid cap.[52] The weight on this component is announced only after bids are collected, but it has remained essentially constant throughout our sample period, so we treat it as known.

An example menu The mechanism implies a menu of payments for each contract at each score. These menus differ by observable characteristics of landowners due to asymmetry in the existing rule. Table B.3 describes an example menu.

[52]We observe bunching at the kink points, suggesting that bidders understand the scoring rule and make sophisticated choices in the mechanism.

Table B.3: Payments (for a Given Target Score) and Market Shares Across Contracts

	Average payment at chosen score	Market share	Average payment at chosen score	Market share	Average payment at chosen score	Market share
	No upgrade		+ wildlife flood plot		+ pollinator habitat	
Intro Grasses 1	25.02	0.140	31.90	0.015	50.36	0.007
Intro Grasses 2	72.47	0.104	76.13	0.022	84.45	0.020
Native Grasses 1	40.61	0.067	46.60	0.005	62.53	0.010
Native Grasses 2	79.36	0.201	82.00	0.023	88.86	0.057
Trees 1	63.05	0.039	67.52	0.003	77.87	0.000
Trees 2	93.31	0.020	95.04	0.003	100.07	0.001
Trees 3	71.49	0.012	74.79	0.001	83.51	0.000
Trees 4	77.87	0.002	80.79	0.000	88.17	0.000
Trees 5	96.74	0.029	98.43	0.003	103.32	0.001
Habitat 1	73.48	0.032	77.01	0.006	85.06	0.001
Habitat 2	80.10	0.039	82.67	0.007	89.37	0.014
Rare Habitat	91.63	0.077	93.39	0.009	98.51	0.025

Notes: Table presents the menu of all 36 possible contracts, split into 12 primary covers and three upgrade options. Table reports payments across contracts, calculated as the rental rate per acre per year to reach a given score (held fixed in this table at the observed score) with a given contract. Payments vary across bidders with heterogeneous $\mathbf{z}_i^s$; this table calculates the averages across all bidders. Table also reports the market shares of each contract.

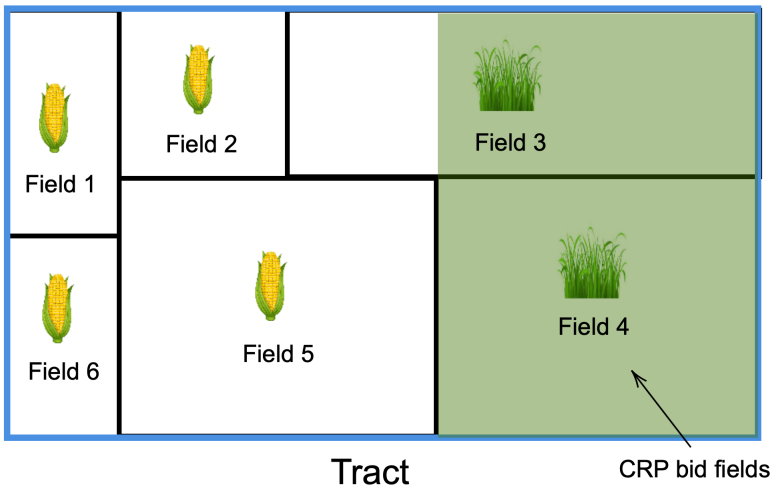
C Data Appendix

Agricultural Units: Tracts and Fields All agricultural land is the US is divided into fields, or Common Land Units, by the USDA. A field is defined as the smallest unit of land that has: (i) a permanent, contiguous boundary, (ii) a common land cover and land management, and (iii) a common owner.[53] There are 37,480,917 fields in the US (as of 2016), with an average size of 33.82 acres. Each field, by definition, has a single land use.

A tract is a collection of fields under one common ownership that is operated as a farm or part of a farm (a tract is a landowner, or bidder, in our setting). The average tract includes 4.75 fields. Each tract can submit at most one bid into a CRP auction. This bid can include any subset of a tract's fields. A bid is not constrained to bid only entire fields; in principle, a bidder can bid any subset of their land, regardless of field delineations. In practice, a large share of bids follow field boundaries, as illustrated by Figure C.2. In our analyses, we therefore treat bid fields as defining the land offered into the mechanism.

Our dataset includes an identifier and the geolocation of each of the bidding tracts, and their subset fields, for all auctions. We only observe the identifiers of the bid fields in 2016. Figure C.1 provides an illustrative example of the various agricultural land units. Figure C.3a maps the geographic distribution of bids.

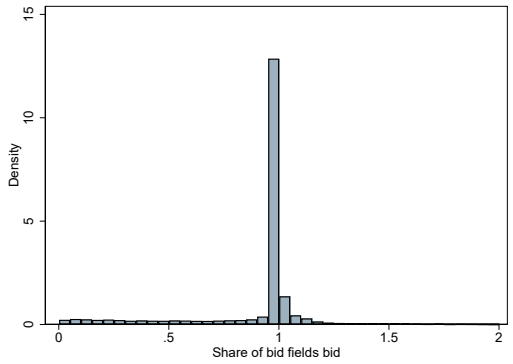
Figure C.1: Example: Tract, Fields, and Bid Fields



Notes: Figure explains the various geographic units in our dataset. The blue outline is a single tract: this is the unit of landowner (bidder) in our analysis. This tract contains six fields, these are administrative delineations of a tract, each with a single land use. The green shaded area represents an example area bid into the CRP. This could follow field boundaries (as for field 4) or cut into fields (as for field 3).

[53] See the Common Land Unit Information Sheet published by the USDA for more details.

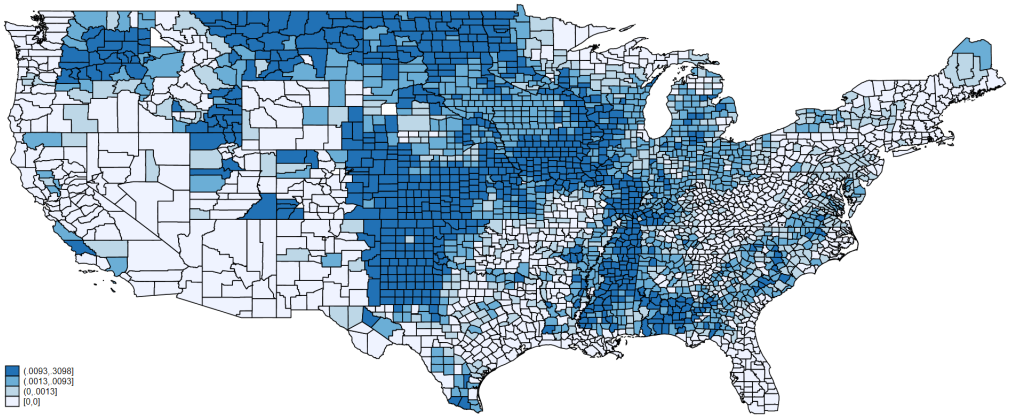
Figure C.2: Share of Bid Fields Bid into the Mechanism



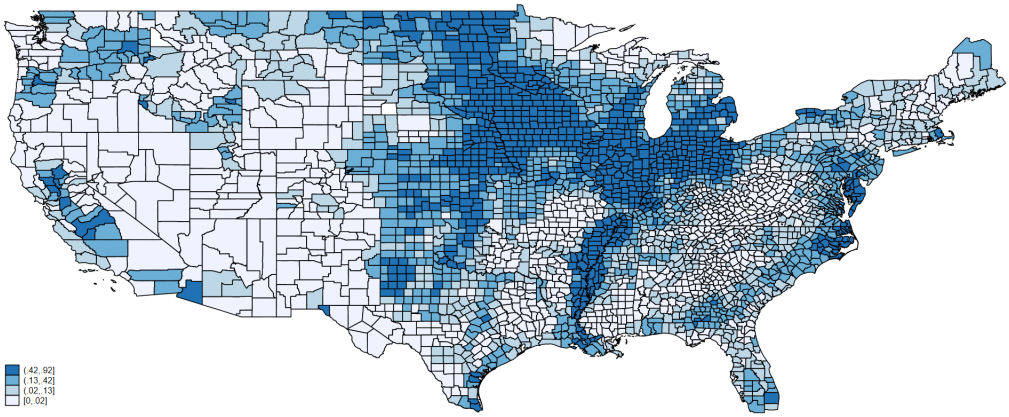
Notes: Figure shows a histogram of the share of the land of the bid fields that are bid into the CRP (the shaded green area as a share of the total area of fields 3 and 4 in Figure C.1). The mass point at one indicates that the vast majority of bidders bid the entire field.

Figure C.3: Maps

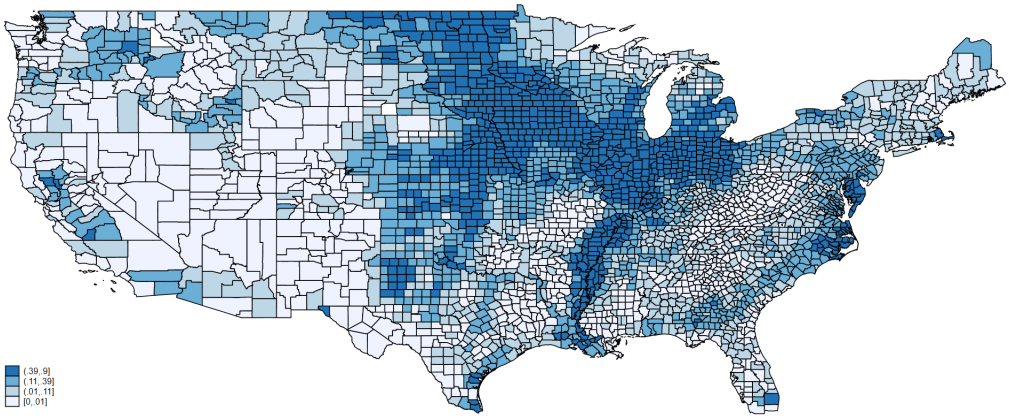
(a) Share of Land Bid for CRP Contract



(b) Share of Land Cropped (Remote Sensing)



(c) Share of Land Cropped (Admin)



Notes: Panel (a) presents the share of land on agricultural tracts that bid for a CRP contract, by county. Panels (b) and (c) plot the share of land cropped on agricultural tracts by county, using the remote sensing (CDL) and admin (Form 578) data, averaged across the years in which auctions occurred. Crop classifications follow Lark et al. (2017) and exclude alfalfa and hay.

Remote Sensing Data (CDL) Our first source of land use data is the Cropland Data Layer (CDL) from 2009 to 2020. The CDL is derived from annual satellite imagery at a 30m by 30m resolution (approximately one quarter acre) for the entire contiguous US. The dataset classifies each pixel into over 50 crop categories and over 20 non-crop categories. The CDL is produced by the National Agricultural Statistics Service (NASS), and is trained on administrative data submitted to the USDA for crop insurance purposes (Form 578, discussed in more detail below).[54]

Our primary analysis aggregates CDL classifications into super-classes of crop versus non-crop, following (Lark et al., 2017). Also following Lark et al. (2017), our crop classification excludes alfalfa, hay, fallow, and idle cropland. The super-class accuracy of the CDL is high with $> 95\%$ average producer's (classified as cropped when truly cropped) and user's (truly cropped when classified as cropped) accuracy in the years 2008-2016 (Lark et al., 2017). Despite this high super-class accuracy, remote sensing classifications are subject to measurement error in classification (Alix-Garcia and Millimet, 2022; Torchiana et al., 2024), particularly when analyzing land use transitions. Moreover, in order to improve accuracy, some states in some years use prior years' CDL as an input into the training algorithm, providing a further source of bias stemming from the classification algorithm.

We merge the CDL to a shapefile of all agricultural fields in the US, which we can then aggregate to landowners (tracts) using USDA identifiers. We merge the CDL data to the geocoded location of the bidder, time-stamped at the point of bidding. Calculating land use outcomes at the tract level as either the share of pixels that fall into the crop super-class, or a weighted average of field-level (binary) cropping indicators produce similar results. We use the former in our main specifications. Figure C.3b maps the geographic distribution of cropland, as measured by the CDL.

Form 578 Administrative Data Our second source of data (from Form 578) is the administrative data submitted to the USDA that the CDL is trained on. The data consist of annual field-level reports of total acreage cropped in detailed crop categories and enrollment in USDA programs. Though Form 578 is self-reported, crop insurance payouts depend on these reports. Unlike the CDL, which has coverage over the entire US, field-level data is only submitted if there is an incentive to do so, i.e. if it is cropped and covered by crop insurance. We assume that all non-reporting fields are not cropped. This is the primary limitation of the administrative data relative to the CDL. Figure C.3c maps the geographic distribution of cropland, as measured by the Form 578 data.

We merge the Form 578 administrative data to bidders based on field and tract identifiers. The USDA administrative data do not include consistent panel identifiers. We therefore construct a panel that tracks changes in field identifiers over time using their geolocation. This is further reason why we prefer the CDL as our baseline data source.

NAIP Imagery Our final dataset is derived from the National Agriculture Imagery Program (NAIP) collected via Google Earth Engine. The NAIP is administered through the Forest Service

[54] See `https://www.nass.usda.gov/Research_and_Science/Cropland/SARS1a.php` for more details and Metadata.

Agency (FSA) of the USDA, and collects 0.6-1m resolution images of all agricultural land during growing season. We obtain NAIP images for enrolled land (the highlighted green area in Figure C.1) to assess compliance with CRP rules. We use high-resolution photographs as classification error in the derived (CDL) data product would mechanically bias toward finding non-compliance.

Figure C.4: Sample Images

(a) Enrolled field



(b) Cropped field



Notes: Example images for classification. For compliance with data privacy, neither of these are actual images of CRP enrolled fields.

Validating Compliance To assess compliance, we hired and trained two MIT undergraduates (the "reviewers") to classify high resolution aerial photographs (NAIP images) of fields at 1m resolution (see Figure C.4 for examples). We focus on the 2016 auction and images taken between 2017 and 2021. Before asking the reviewers to classify any images, we provided them with a test set of hundreds of images of cropped and uncropped fields across the US. The reviewers used this test set to familiarize themselves with the visual patterns of cropped fields (see Figure C.4b). We then provided each of the reviewers with over 1,000 images of CRP enrolled fields and hundreds of placebo cropped fields as attention checks. The reviewers were blind to whether the images were of CRP enrolled fields or placebo cropped fields. Each of the two reviewers were provided with the same images.

Table C.1 presents results for the classification exercise. We restrict to the 83% of CRP images that the reviewers agreed upon for our assessment of compliance to minimize the potential for classification error. We find only 5% of fields to be out of compliance in all post-period years. Once we drop the two "transition" years from 2017-2018, we find even lower rates of non-compliance, and reject rates of non-compliance above 3%. We attribute the difference between columns (1) and (2) to be driven by the fact that fields appear different when they are transitioning out of cropland,

e.g. rows from row cropping may still be visible as new vegetation grows in. Rates of cropping are classified as substantially higher, at approximately 40%, on placebo cropped fields indicating that the reviewers were making meaningful classifications. We note, however, that this number is far below 100%. This is because we instructed the reviewers to be conservative in their assessment of non-compliance, operating under the null hypothesis that the program is enforced.

An important caveat is that this exercise only studies compliance on the base action, land retirement, not the top-up actions, which we cannot observe. We thus use this assessment of compliance to make an inference about the overall compliance regime.

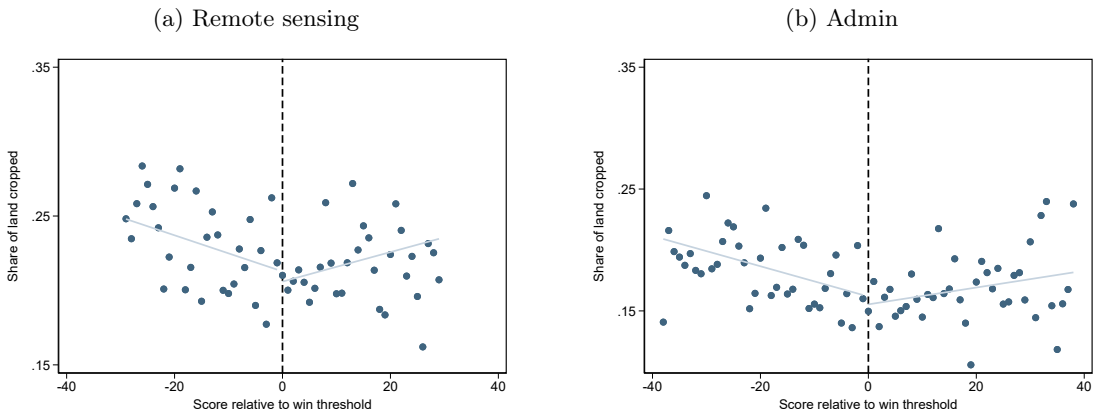
Table C.1: Validation of Compliance

	All post-period years	Drop first two years
	(1)	(2)
Share of contracted fields classified as cropped	0.054	0.024
	(0.008)	(0.005)
Upper bound of 95% CI	0.070	0.034
N fields classified (with agreement)	925	842
Rate of agreement across reviewers	0.825	0.863

Notes: Table presents results from an exercise classifying aerial photographs of contracted fields as cropped or non-cropped among two reviewers, who also reviewed images of non-CRP fields and were blind to the distinction. Classification focuses on the 2016 auction. Column (1) includes photographs from 2017-2021. Column (2) includes only photographs from 2019-2021. Crop classifications are based on only fields in which the two reviewers agree (which occurred for 83-86% of fields). Fields more likely to be flagged as non-compliant (based on remote sensing data) were over-sampled, to be as conservative as possible.

D Supplemental Figures and Tables

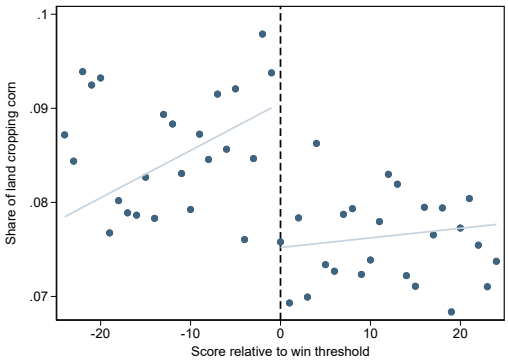
Figure D.1: Spillovers: Cropping on Non-Bid Fields



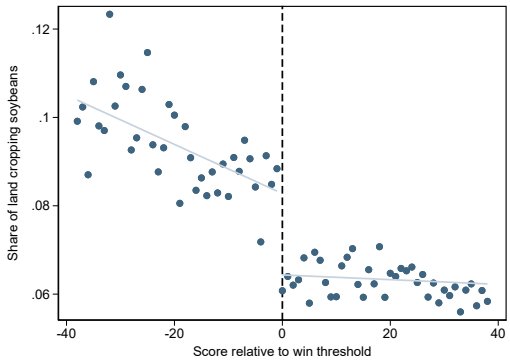
Notes: Panels (a) and (b) present raw data and estimates from equation (7) for $r(i,t) > 0$ (post-auction). Regression is estimated at the bidder level, restricting to non-bid fields among bidding landowners. Estimates are restricted to the 2016 auction where delineations of bid and non-bid fields are observed. Land-use outcomes are measured as the share of the bidding land that is cropped using the remote sensing data (a) and administrative data (b). The running variable is the difference between each bidder's score and the threshold score. Positive numbers on the x-axis correspond to winning scores, negative numbers correspond to losing scores. Each observation is a bidder-year. Corresponding coefficient estimates and standard errors presented in Table 2.

Figure D.2: Additional RD Plots: Remote-Sensing Data

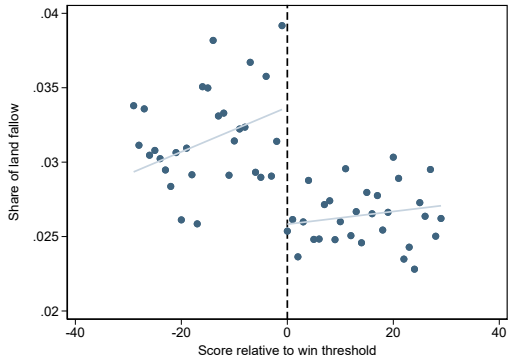
(a) Cropping corn



(b) Copping soybeans

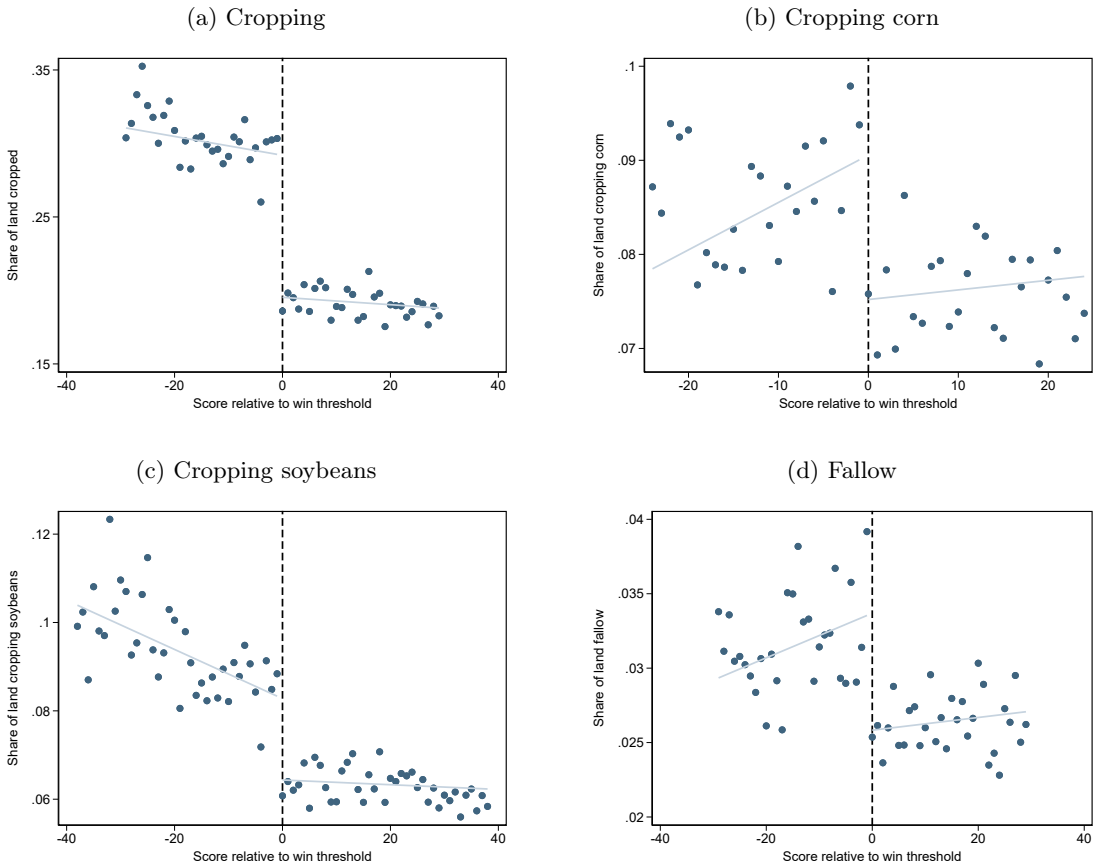


(c) Fallow



Notes: Figure presents raw data and estimates from equation (7) for $r(i,t) > 0$ (post-auction). Land-use outcomes are measured using crop classifications in the remote sensing data. The running variable is the difference between each bidder's score and the threshold score. Positive numbers on the x-axis correspond to winning scores, negative numbers correspond to losing scores. Each observation is a bidder-year. Corresponding coefficient estimates and standard errors presented in Table 2.

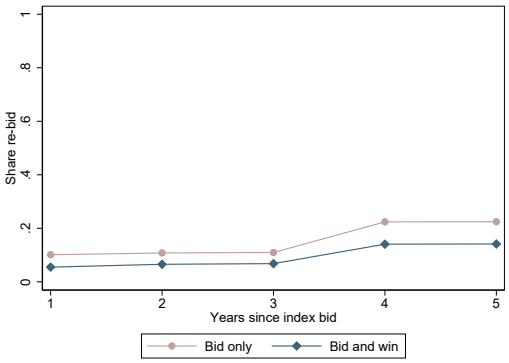
Figure D.3: Additional RD Plots: Admin Data



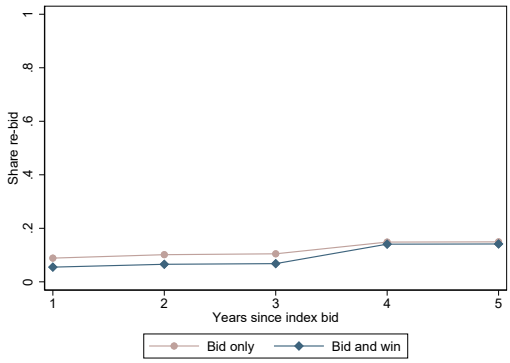
Notes: Figure presents raw data and estimates from equation (7) for $r(i,t) > 0$ (post-auction). Land-use outcomes are measured using crop classifications in the Form 578 data reported to the USDA. The running variable is the difference between each bidder's score and the threshold score. Positive numbers on the x-axis correspond to winning scores, negative numbers correspond to losing scores. Each observation is a bidder-year. Corresponding coefficient estimates and standard errors presented in Table 2.

Figure D.4: Re-bidding Hazard

(a) All losing bidders



(b) Losing bidders near winning score threshold



Notes: Figure plots the share of losing bidders who have rebid at least once in the years following an index auction, split by all bidders (beige) and successful bidders (blue). Panel (a) includes all losing bidders. Panel (b) restricts to bidders near (within 25 points) of the winning score threshold.

Table D.1: RD Estimates: By Win Threshold of Bid Rental Rate for Base Contract

	Remote-sensing		Admin	
	Effect on share cropped	Additionality	Effect on share cropped	Additionality
	(1)	(2)	(3)	(4)
Quartile 1 threshold bid (lowest)	-0.039	0.139	-0.064	0.227
	(0.013)		(0.014)	
Quartile 2 threshold bid	-0.059	0.190	-0.072	0.231
	(0.012)		(0.013)	
Quartile 3 threshold bid	-0.031	0.126	-0.046	0.185
	(0.012)		(0.013)	
Quartile 4 threshold bid (highest)	-0.075	0.403	-0.094	0.507
	(0.015)		(0.015)	

Notes: Table presents pooled RD coefficients (Equation (7) for $r(i,t) > 0$ (post-auction) split by the bid rental rate required to achieve the threshold score with the base contract (quartiles). Columns (1) and (3) present estimates of the share of bidders' land that is cropped, and columns (2) and (4) present implied additionality estimates based on the share of bidders' land that obtains a CRP contract (in that quartile). This parameterizes heterogeneity in the location of the discontinuity across auctions and variation within auctions across bidders (based on $\mathbf{z}_i^s$). Standard errors clustered at the bidder level.

Table D.2: RD Estimates by Auction

	Share cropped		Share of land contracted	Additionality		Share awarded contract
	Remote sensing	Admin		Remote sensing	Admin	
	(1)	(2)	(3)	(4)	(5)	(6)
Most restrictive: 2016	-0.048	-0.079	0.389	0.122	0.204	0.185
	(0.016)	(0.015)	(0.013)			
2011	-0.068	-0.089	0.396	0.173	0.226	0.775
	(0.012)	(0.013)	(0.008)			
2013	-0.064	-0.106	0.323	0.197	0.329	0.870
	(0.016)	(0.017)	(0.009)			
2012	-0.077	-0.104	0.355	0.217	0.294	0.877
	(0.014)	(0.015)	(0.011)			
Least restrictive: 2010	-0.109	-0.120	0.261	0.416	0.461	0.918
	(0.020)	(0.020)	(0.011)			

Notes: Table presents RD coefficients (Equation (7) for $r(i,t) > 0$ (post-auction) for each of the five auctions with post-period land use data. Each row is an auction, ordered by the share awarded contracts. Columns (1)-(2) present estimates of the share of bidders' land that is cropped (measured in the remote sensing data and admin data), column (3) presents estimates of the share of land covered by a CRP contract, columns (4)-(5) report implied additionality estimates. Column (6) reports the share awarded a contract. Standard errors clustered at the bidder level.

Table D.3: RD Coefficient Estimates: Weighted by CRP Acreage Offered

	Remote sensing (1)	Admin (2)
Panel A: Share of land cropped vs. contracted		
Share of land cropped pre-auction (placebo)	0.010	0.021
	(0.007)	(0.013)
Share of land cropped post-auction (pooled)	-0.115	-0.153
	(0.008)	(0.008)
Share of land cropped post-auction (average year effects)	-0.122	-0.157
	(0.008)	(0.008)
Share of land contracted post-auction	0.544	
	(0.006)	
Panel B: Other outcomes		
Share of land cropped corn	-0.020	-0.029
	(0.003)	(0.003)
Share of land cropped soybeans	-0.025	-0.034
	(0.003)	(0.003)
Share of land fallow	-0.015	-0.024
	(0.002)	(0.002)
Share of land in natural vegetation or grassland	0.143	
	(0.009)	
Observations in 25-point window		
N bidders	41,269	41,269
N bidder-years	495,228	288,883

Notes: Table presents coefficient estimates from equations (6) and (7) with land use outcomes measured in the remotely sensed (column (1)) and administrative (column (2)) data, weighted by the CRP offered acreage share. All results use a local linear regression on either side of the win threshold in the MSE-optimal bandwidth (Calonico et al., 2014). All estimates are from equation (7), except the "average year effects" row, which presents the average of the post-period year effects (coefficient estimates of $\beta_{r(i,t)}$ from (6)) weighting each year equally. The pooled post-period includes an average of 7-8 post-auction years. Natural vegetation or grassland is only observed in remotely sensed data. Share of land contracted post auction estimates the share of bidders' land contracting among winning bidders. Standard errors are clustered at the bidder level. Estimates of additionality are calculated by dividing the estimates for the share of land cropped by the estimates of the share of land contracted and equal 21-22% (remote sensing) and 28-29% (admin). Estimates using the share of land in natural vegetation or grasslands yields a similar estimate (26%).

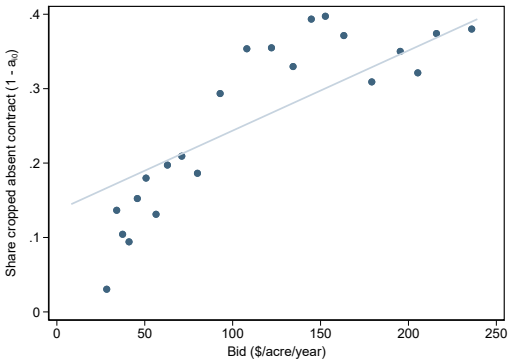
Table D.4: RD Coefficient Estimates | Bid $\geq$ Five Acres of Land

	Remote sensing (1)	Admin (2)
Panel A: Share of land cropped vs. contracted		
Share of land cropped pre-auction (placebo)	0.005	0.006
	(0.006)	(0.010)
Share of land cropped post-auction (pooled)	-0.076	-0.102
	(0.007)	(0.006)
Share of land cropped post-auction (average year effects)	-0.083	-0.106
	(0.007)	(0.007)
Share of land contracted post-auction	0.345	
	(0.004)	
Panel B: Other outcomes		
Share of land cropped corn	-0.016	-0.022
	(0.003)	(0.003)
Share of land cropped soybeans	-0.021	-0.026
	(0.003)	(0.003)
Share of land fallow	-0.009	-0.014
	(0.002)	(0.002)
Share of land in natural vegetation or grassland	0.097	
	(0.007)	
Panel C: Spillovers to non-bid fields		
Share of non-bid fields cropped	-0.007	-0.007
	(0.012)	(0.011)
Observations in 25-point window		
N bidders	37,776	37,776
N bidder-years	453,312	264,432
Spillovers (bid fields observed): N bidders	6,770	6,770
Spillovers (bid fields observed): N bidder-years	81,240	47,390

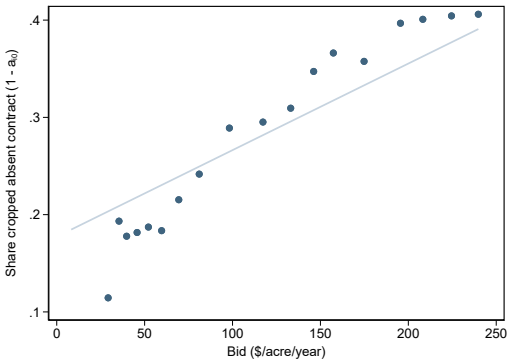
Notes: Table presents coefficient estimates from equations (6) and (7) with land use outcomes measured in the remotely sensed (column (1)) and administrative (column (2)) data, restricted to bidders who bid more then five acres into the mechanism (following Lark et al. (2017)). All results use a local linear regression on either side of the win threshold in the MSE-optimal bandwidth (Calonico et al., 2014). All estimates are from equation (7), except the "average year effects" row, which presents the average of the post-period year effects (coefficient estimates of $\beta_{r(i,t)}$ from (6)) weighting each year equally. The pooled post-period includes an average of 7-8 post-auction years. Natural vegetation or grassland is only observed in remotely sensed data. Share of land contracted post auction estimates the share of bidders' land contracting among winning bidders. Standard errors are clustered at the bidder level. Estimates of additionality are calculated by dividing the estimates for the share of land cropped by the estimates of the share of land contracted and equal 22-24% (remote sensing) and 30-31% (admin). Estimates using the share of land in natural vegetation or grasslands yields a similar estimate (28%).

Figure D.5: Testing for Asymmetric Information, Admin Data

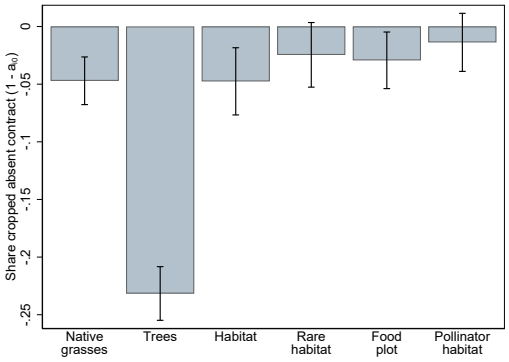
(a) Additionality vs. bids



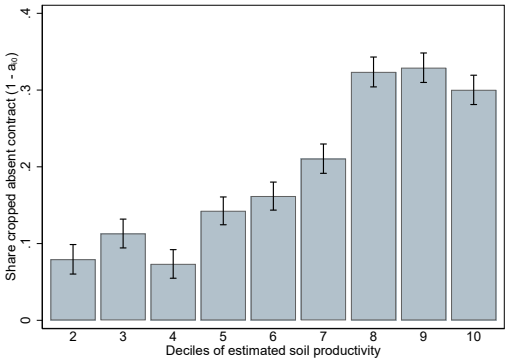
(b) Additionality vs. bids | observables



(c) Additionality across contracts

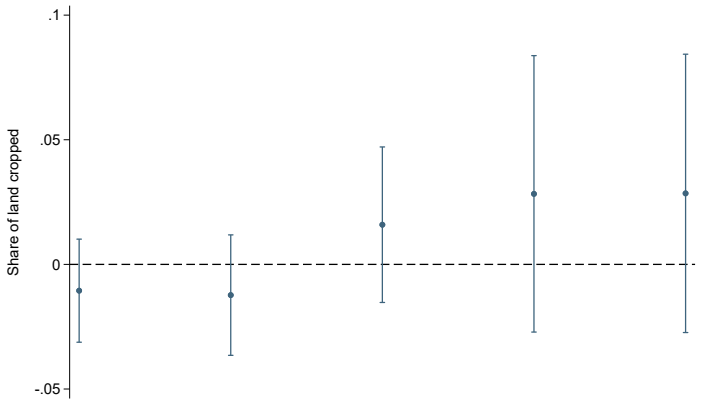


(d) Observable predictors of additionality



Notes: Figures present estimates from regression specifications in equation (8). Regressions in all panels control for landowner characteristics in the scoring rule: whether a bidder is in a wildlife priority zone, estimates of groundwater quality, estimates of surface water quality, estimates of wind and water erosion (deciles), air quality impacts, and whether or not a bidder is in an air quality zone. The outcome variable in all panels is a landowner-specific measure of additionality, calculated as the share of all fields bid into the CRP mechanism that are cropped post auction for rejected landowners. The sample is restricted to the 2016 auction, in which 82% of bidders are rejected and the delineations of bid fields are observed. Cropping on bid fields is measured in 2017-2019 in the administrative data, with each field and year equally weighted. Panel (a) is a binned scatterplot correlating the dollar bid (per acre, per year) with additionality, conditional on characteristics included in the scoring rule. Panel (b) adds controls for interaction terms of prior land use (quartiles of share of land cropped prior to bidding and re-enrolling CRP status) and deciles of estimated soil productivity. Panel (c) plots relative additionality by the chosen contract in the bid, relative to an omitted category of introduced grasses, conditional on characteristics included in the scoring rule. Panel (d) plots relative additionality by deciles of estimated soil productivity, conditional on characteristics included in the scoring rule. Standard errors clustered at the bidder level.

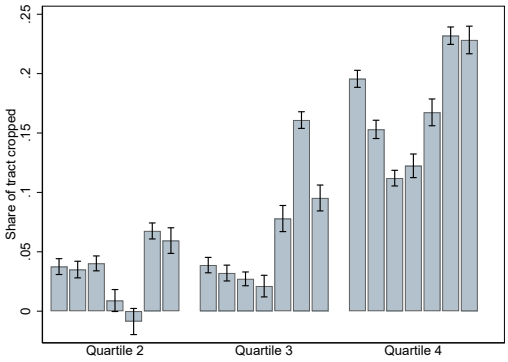
Figure D.6: RD Estimates: Tree-Related Contracts



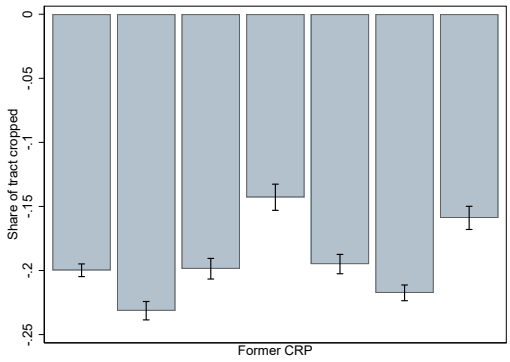
Notes: Figures presents RD coefficients (Equation (7) for $r\left(i,t\right)>0$ (post-auction) for each of the five auctions with post-period land use data, restricted to bids for tree-related contracts. Each estimate is an auction, ordered over time from left to right. The outcome is the share of bidders' land that is cropped (measured in the remote sensing data). Standard errors clustered at the bidder level. F statistic testing joint equality of coefficients across auctions (restricting to bids for tree contracts): 0.64.

Figure D.7: Tract-level Heterogeneity Across Auctions

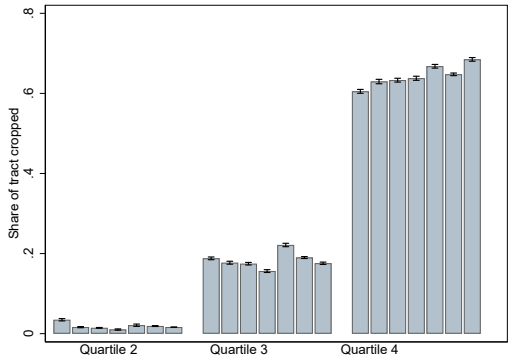
(a) By Estimates of Soil Productivity



(b) By Former CRP



(c) By Prior Cropping Share

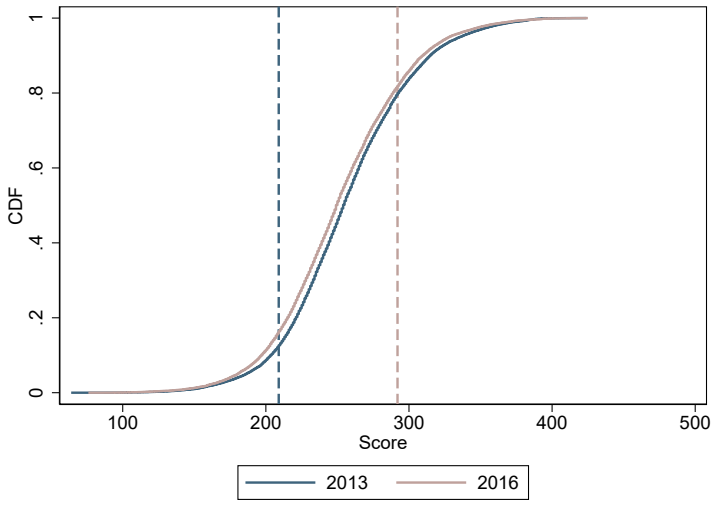


Notes: Figures present tract-level heterogeneity in cropping rates (measured in the remote sensing data) for $r(i,t) = 0$ (and $r(i,t) = -1$ for the 2021 auction, to be able to compare all seven auctions) across observable characteristics, by auction, ordered over time from left to right. Cropping rates reported relative to the omitted category: the lowest quartile of soil productivity (a), a new CRP participant (b), and the lowest quartile of share cropped prior to bidding (c). Standard errors clustered at the bidder level. F statistics testing joint equality of coefficients across auctions: 111 (a), 61 (b), 67 (c).

E Model and Estimation Details

Figure E.1 provides empirical support for the assumed uncertainty in quantity cleared. Each Farm Bill specifies the *total acreage* that can be covered by CRP contracts at a given point in time. The quantity cleared in the auction is therefore determined jointly by the Farm Bill and prior contract expirations. It can vary substantially in ways that may not be obvious to bidders submitting their bids. To demonstrate this, we compare the 2013 and 2016 auctions. These two auctions had very different quantity thresholds, and thus very different threshold scores, denoted by the dashed lines in blue and beige. However, consistent with bidder uncertainty about the ex-post threshold score, the cumulative distribution functions (CDFs) of bidder scores across the two auctions are similar.

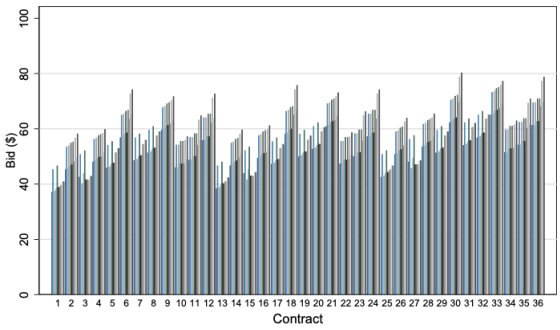
Figure E.1: CDF of Scores versus Winning Thresholds: 2013 versus 2016



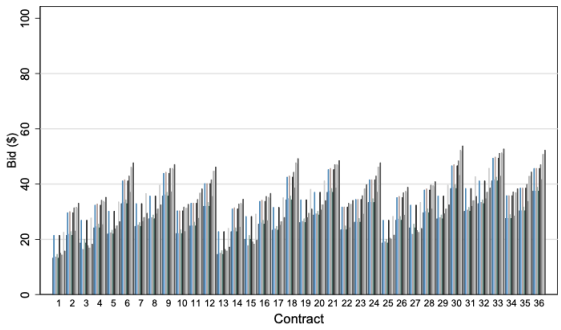
Notes: Figure presents ex-post win thresholds and cumulative distribution functions (CDFs) of ex-ante score distributions for the 2013 and 2016 auctions.

Figure E.2: Scoring Rule Variation: Summarized

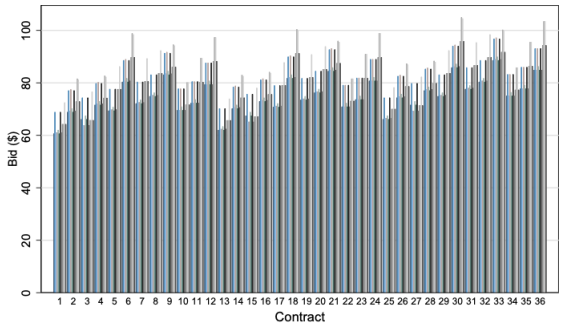
(a) Target 2016 Threshold Score



(b) Target 1st Percentile Score



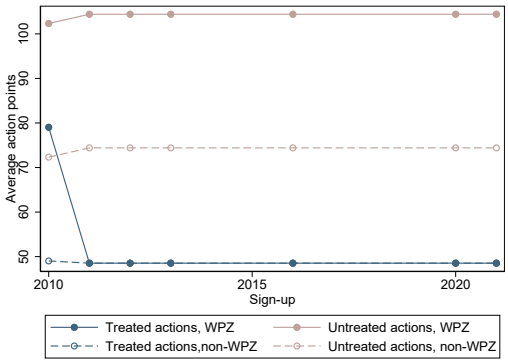
(c) Target Average Threshold Score



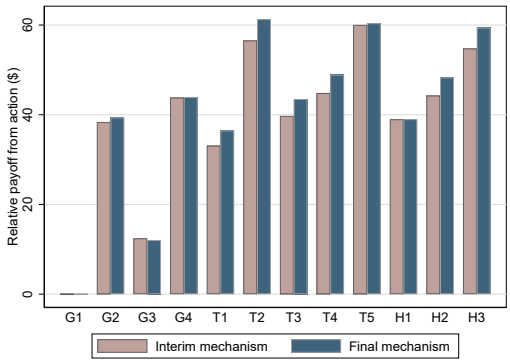
Notes: Figure presents sources of policy variation in the scoring rule by plotting the dollar bid (per acre, per year) required to reach a target score across all 36 contracts across variations of the scoring rule (see also Figure E.3). Conversion of points to bids at the threshold score calculated for a landowner with average land-based points and rate of substitution between points and dollar bids (abstracting from the kinked incentives in points bidders receive as a percentage of their bidcap, see Appendix F for more detail). Each set of 36 colored vertical bars represents a different variation of the scoring rule. Panels (a), (b), and (c) present the same sources of variation at the levels associated with different target scores: the 2016 threshold score (a), the lowest percentile score (b), and the average non-2016 threshold score (c).

Figure E.3: Specific Sources of Variation in the Scoring Rule

(a) Wildlife Priority Zone Variation



(b) Mid-Mechanism Policy Change

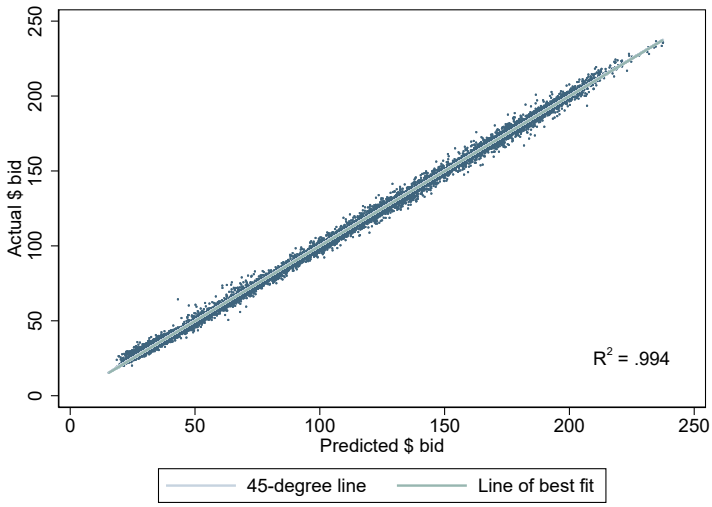


Notes: Figure presents sources of policy variation in the scoring rule that yield variation in payments across contracts differentiated by top-up conservation actions. Panel (a) plots average action points awarded for a set of "treated" actions, actions for which after the 2011 auction WPZ bidders no longer got WPZ points, and "untreated" actions, whose points remained the same, and the same average action points for non-WPZ bidders. Panel (b) plots the average rental rate that would be received for a target score among bidders under the interim mechanism before the introduction of Climate Smart Practice Incentives, and in the final mechanism after their introduction, for each of the twelve primary covers. G indicates grasses, T indicates trees, H indicates habitats.

Estimation

Step 0: Constructing the Scoring Rule We only observe scores for chosen bids $\mathbf{b}_i$, so we construct the function $s\left(\mathbf{b}_i, \mathbf{z}_i^s\right)$ from the EBI Factsheets. Figure E.4 confirms that our reconstruction performs well: at observed actions, our scoring-rule-implied required bid rental rate to achieve the score chosen in the data predicts the observed bid rental rate with an R^2 of over 0.99.

Figure E.4: True versus Predicted Bid Rental Rate at Observed Scores and Contracts



Notes: Figure presents a scatter plot of true versus predicted bid rental rates at observed contract and score choices to validate the construction of $s\left(\mathbf{b}_i, \mathbf{z}_i^s\right)$. Each dot represents 11 observations (per disclosure requirements).

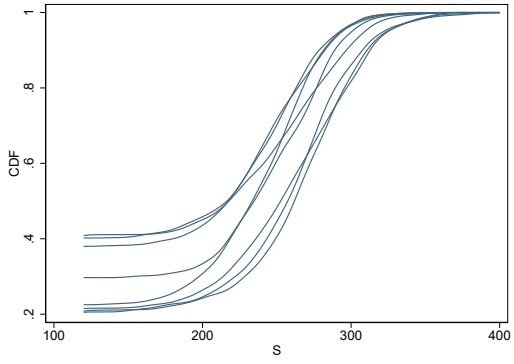
Step 1: Obtain Bidder Beliefs via Simulation Our resampling procedure to simulate the probability of winning at any score, $G(S)$ follows Hortaçsu (2000); Hortaçsu and McAdams (2010). Specifically, we:

1. Fit a Beta distribution to the observed distribution of acreage thresholds across auctions. For this step, we use additional historic data on auctions starting in 2000. This provides us with 11 auctions.
2. Fit a Beta distribution to the observed distribution of number of opposing bidders across auctions. For this step, we again use additional historic data on auctions starting in 2000. This provides us with 11 auctions.
3. Draw an acreage threshold from the distribution fit in Step 1 and the number of opposing bidders, N, in Step 2. Then, for each auction g, sample with replacement N bidders from the empirical distribution of bidders in that auction. Given the joint distribution of scores and acreage amounts among the N resampled bidders, and the drawn acreage threshold, find the winning score threshold S.
4. Repeat Step 3 and obtain an auction specific probability of winning at any given score $G_g(S)$ using a kernel density fit to the distribution of simulated winning scores.[55]

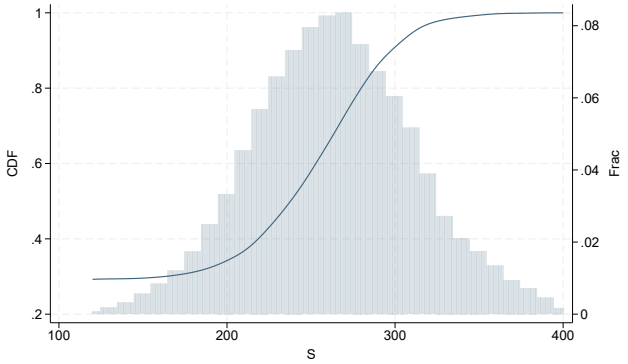
Bidders form expectations about the distribution of competing scores without knowledge of their competitors' identities or characteristics, consistent with the large and decentralized bidding process, so $G_g(S)$ is the same for all bidders. Figure E.5 plots the output of our simulation procedure for each auction (a) and compares the average CDF (across auctions) to the overall empirical score distribution (b).

Figure E.5: Probability of Winning at Score S

(a) $G(S)$ across auctions



(b) $G(S)$ vs. empirical score distribution



Notes: Figure presents CDFs of the simulated distribution of win probabilities at a given score across auctions (a) and on average versus the average empirical score distribution (b).

[55] We use a Gaussian kernel and a bandwidth of 5 points.

We assume that bidders are able to form expectations about the distribution of competing scores. This might be challenging when the distribution of scores changes across auctions. To assess the implications for our estimates, we re-estimate costs using beliefs based on the empirical distribution in the prior auction (versus the current auction, as in baseline). Table E.1 compares results.

Table E.1: Mean Landowner Costs of Accepting CRP Contracts under Alternative Beliefs

	Current auction beliefs		Prior auction beliefs	
	All	Bidders with > median soil productivity	All	Bidders with > median soil productivity
	(1)	(2)	(3)	(4)
Base cost (c_i)	67.19	90.86	69.57	97.69
Top-up cost (κ_{ij})				
Native grasses	0.02	3.91	0.17	4.50
Trees	23.57	26.96	23.76	27.20
Habitat	15.05	18.34	14.93	18.29
Rare habitat	15.59	19.07	15.68	19.24
Wildlife food plot	18.87	15.34	18.80	15.10
Pollinator habitat	18.18	17.56	20.79	18.33

Notes: Table presents estimated mean landowner costs for the base cost c_i and top-up cost κ_{ij} in dollars per acre per year. The base contract of introduced grasses is normalized to zero. The cost of each contract j is defined as $c_i + \kappa_{ij}$. Costs are estimated using revealed preferences in optimal bidding (equation (10)) given beliefs from the baseline resampling procedure (columns (1) and (2)) and a modified resampling procedure where the distribution of competing bidders from the prior auction is used (columns (3) and (4)). Columns (1) and (3) presents mean costs for all bidders across all auctions (excluding the first auction) and columns (2) and (4) restricts to bidders with above median soil productivity.

Step 2: Estimate $F_{c,\kappa\,|\,\mathbf{z}}$ Our estimation procedure is as follows:

1. **Construct a proposal distribution.** We begin by constructing a proposal distribution from which to draw proposal (c_i, κ_i) draws. We obtain our proposal distribution by estimating a simplified version of the model. Bidders choose a score using only their *expectations* of their κ_{ij} draws, then given that score, choose an optimal contract. In this model, estimation of κ_{ij} and c_i can be separated into a discrete choice problem and an inversion. We obtain parameter estimates from this simplified model, then set our proposal distribution to be independent normals with the estimated means and variances of this simplified model.

2. **Draw from proposal and solve the bidder's problem.** Following the approach of Ackerberg (2009), we use a change of variables to draw simulations of $\left(c_i^k, \kappa_i^k\right)$ from the proposal distribution and solve the bidder's problem in equation (10) for each bidder and each simulation draw. Bidders can only bid integer scores, so to solve equation (10), we search over all feasible score-contract combinations among integers in the support of observed scores. This change of variables allows us to solve the bidder's problem only $N \times K$ times, once for each bidder and each simulation draw, instead of $N \times K \times R$ times, for each evaluation of the objective function (R times).

3. **Coarsen choice probabilities.** Because the number of possible bids is large (on the order

of 10,000 choices), we face the challenge that the probability of simulating each bid observed in the data is low. We address this challenge by coarsening the bidder's solution obtained in Step 2. We coarsen to the cartesian product of (i) deciles of the scoring rule and (ii) the five dimensions of p_j when u_j is the no upgrade option, plus the two upgrade options. Let $\widetilde{\mathbf{b}}_i^* = \left(\tilde{S}_i, \tilde{\mathbf{x}}_i\right)$ denote the optimal coarsened bid observed in the data.

4. **Reweight simulation draws.** We can then construct the importance sampling estimator by re-weighting simulation draws. The likelihood of observing the coarsened choice in the data, $\widetilde{\mathbf{b}}_i^* = \left(\tilde{S}_i, \tilde{\mathbf{x}}_i\right)$, given a parameter guess θ, is:

$$\mathcal{L}_i = \frac{1}{K} \sum \mathbb{1}\left(\widetilde{\mathbf{b}}_i^* = \widetilde{\mathbf{b}}_i^{*k} | \left(c_i^k, \kappa_i^k\right)\right) \frac{p\left(\left(c_i^k, \kappa_i^k\right)|\theta\right)}{g\left(\left(c_i^k, \kappa_i^k\right)\right)}, \tag{21}$$

where $\widetilde{\mathbf{b}}_i^{*k}$ is the coarsened optimal bid given simulation draw $\left(c_i^k, \kappa_i^k\right)$, the solution to the bidder's problem in equation (10), and the coarsening described in Step 3. Equation (21) then re-weights simulation draws by $\frac{p\left(\left(c_i^k, \kappa_i^k\right)|\theta\right)}{g\left(\left(c_i^k, \kappa_i^k\right)\right)}$, where $p\left(\left(c_i^k, \kappa_i^k\right)|\theta\right)$ is the probability of observing simulation draw $\left(c_i^k, \kappa_i^k\right)$ given parameter guess θ, and $g\left(\left(c_i^k, \kappa_i^k\right)\right)$ the probability of observing $\left(c_i^k, \kappa_i^k\right)$ given the proposal distribution from Step 1.

5. **Find θ to maximize the log likelihood**. We suppressed dependence in (21) on $\mathbf{z}_i$. We estimate θ separately for each of the 32 cells of observable heterogeneity for a sample of 1,000 bidders in each cell, across auctions (due to computational constraints on the USDA servers). An auxiliary benefit of the importance sampling approach of Ackerberg (2009) is that it yields a differentiable objective function.

6. **Repeat**. We repeat Steps 2-5 several times, using estimates from the solution to Step 5 as the new proposal distribution. Our final estimates use 10,000 simulation draws to mitigate simulation bias.

Table E.2 presents parameter estimates for selected observable cells $\mathbf{z}_i$.

Step 3: Estimate $\tau(\mathbf{z}_i, c_i, \kappa_i)$ Our final step involves estimating the conditional expectation function $\tau(\mathbf{z}_i, c_i, \kappa_i) = \mathbb{E}[1 - a_{i0} \,|\, \mathbf{z}_i, c_i, \kappa_i] = \pi \cdot \mathbf{z}_i + \beta \cdot c_i + \alpha \cdot \kappa_i$. We match model implied moments of additionality to observed moments of additionality, $1 - a_{i0}$, among bidders who lose the auction. We search for $\theta^\tau = (\pi, \beta, \alpha)$ that minimizes $\hat{g}(\theta^\tau)' A \hat{g}(\theta^\tau)$ for weight matrix A (the two-step optimal weight matrix) and $\hat{g}(\theta^\tau) = \hat{\mathbb{E}}\left[m_i - \frac{1}{K}\sum_k m_i\left(\theta^\tau | c_i^k, \kappa_{\mathbf{i}}^{\mathbf{k}}\right)\right]$, where $\hat{\mathbb{E}}$ denotes the sample expectation, for m_i equal to:

- Additionality at the award threshold: $(1 - a_{i0}) \cdot \mathbb{1}\left[\underline{S} - b < s(\mathbf{b}_i^*, \mathbf{z}_i^s) < \underline{S}\right]$ for bandwidth b.
- Additionality by observable characteristics: $(1 - a_{i0}) \cdot \mathbb{1}\left[s(\mathbf{b}_i^*, \mathbf{z}_i^s) < \underline{S}\right] \cdot \mathbf{z}_i$.
- Covariance between additionality and chosen scores: $(1 - a_{i0}) \cdot s(\mathbf{b}_i^*, \mathbf{z}_i^s) \cdot \mathbb{1}\left[s(\mathbf{b}_i^*, \mathbf{z}_i^s) < \underline{S}\right]$.
- Additionality within chosen contracts: $(1 - a_{i0}) \cdot \mathbb{1}[x_{ij} = 1] \cdot \mathbb{1}\left[s(\mathbf{b}_i^*, \mathbf{z}_i^s) < \underline{S}\right]$.

Our estimation approach follows the following steps:

1. Draw simulations $\left(c_i^k, \kappa_i^k\right)$ from $F_{c,\kappa \mid \mathbf{z}}$ estimated in Step 2.
2. Calculate optimal bids $\mathbf{b}_i^*$ given $\left(c_i^k, \kappa_i^k\right)$ using equation (10).
3. Calculate $m_i\left(\theta^\tau | c_i^k, \kappa_i^k\right)$ by replacing $1 - a_{i0}$ with $\pi \cdot \mathbf{z}_i + \beta \cdot c_i + \alpha \cdot \kappa_i$ and observed bids with simulated optimal bids for each simulation draw k and parameter guess θ^τ.
4. Minimize the objective $\hat{g}\left(\theta^\tau\right)' A \hat{g}\left(\theta^\tau\right)$.

Because we require an observation of bid fields to calculate $1 - a_{i0}$, we estimate $\tau\left(\mathbf{z}_i, c_i, \kappa_i\right)$ using only the auction where we observe bid fields (2016). Our primary estimates use the remote-sensing data from 2017-2020 to measure $1 - a_{i0}$. We weight each bidder's field and year equally. This approach relies on the assumption that the relationships estimated in $\tau\left(\mathbf{z}_i, c_i, \kappa_i\right)$ in this auction can be extrapolated to the other auctions in our sample, and that $\tau\left(\mathbf{z}_i, c_i, \kappa_i\right)$ can be estimated in only the four years following the auction. This may seem unappealing given the transition period in Figure 4, but we note that $1 - a_{i0}$ is calculated among losing bidders, not those transitioning into land retirement.

We calculate standard errors via block bootstrap, resampling at the bidder level. We incorporate estimation error in the earlier step by taking a new cost draw from the estimated variance-covariance matrix of the parameters of $F_{c,\kappa \mid \mathbf{z}}$ and re-calculating optimal bids for that draw for each bootstrap sample.

Table E.2: $F_{c,\kappa\,|\,\mathbf{z}}$ Parameter Estimates (Select $\mathbf{z}_i$)

	Former CRP = 0				Former CRP = 1			
Prior crop	Q1	Q2	Q3	Q4	Q1	Q2	Q3	Q4
Soil prod.	Q1	Q2	Q3	Q4	Q1	Q2	Q3	Q4
	(1)	(2)	(3)	(4)	(5)	(6)	(7)	(8)
c_i								
Mean	29.82	41.65	64.83	131.94	35.49	44.98	66.34	124.49
	(0.02)	(0.04)	(0.05)	(0.06)	(0.02)	(0.03)	(0.04)	(0.07)
Log σ_c	1.67	2.57	3.49	3.69	1.44	2.47	3.43	3.90
	(0.004)	(0.002)	(0.001)	(0.001)	(0.004)	(0.002)	(0.001)	(0.001)
κ_{ij}								
Means								
Native grasses	0.35	-4.83	4.06	1.62	-4.30	-6.40	5.92	-0.90
	(0.02)	(0.03)	(0.02)	(0.02)	(0.02)	(0.02)	(0.02)	(0.03)
Trees	26.24	25.91	26.62	33.38	13.84	18.77	23.58	31.76
	(0.02)	(0.03)	(0.02)	(0.02)	(0.02)	(0.02)	(0.02)	(0.02)
Habitat	15.95	11.90	16.13	20.53	14.03	12.95	18.89	13.62
	(0.03)	(0.03)	(0.03)	(0.03)	(0.03)	(0.03)	(0.03)	(0.03)
Rare habitat	15.98	14.43	18.50	12.37	18.10	11.84	22.31	16.94
	(0.03)	(0.04)	(0.03)	(0.02)	(0.04)	(0.04)	(0.03)	(0.03)
Wildlife food plot	24.53	24.40	12.38	14.88	23.78	22.78	14.00	17.53
	(0.03)	(0.03)	(0.02)	(0.02)	(0.02)	(0.03)	(0.02)	(0.02)
Pollinator habitat	14.36	10.87	13.65	16.45	21.83	19.52	17.71	19.64
	(0.02)	(0.02)	(0.02)	(0.02)	(0.02)	(0.02)	(0.02)	(0.02)
Log σ_κ	2.60	2.93	2.81	2.70	2.76	2.91	2.80	2.86
	(0.001)	(0.001)	(0.001)	(0.001)	(0.001)	(0.001)	(0.001)	(0.001)

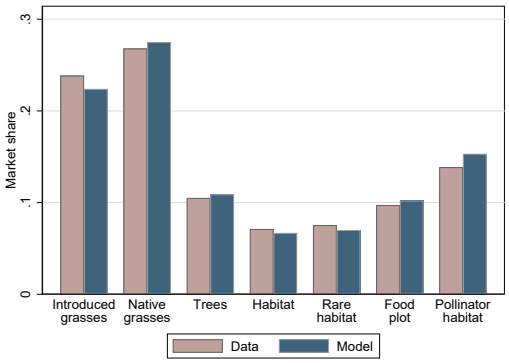
Notes: Table presents presents parameter estimates for 8 cells of $\mathbf{z}_i$. Standard errors calculated using the inverse of the negative Hessian, calculated numerically.

Model Fit

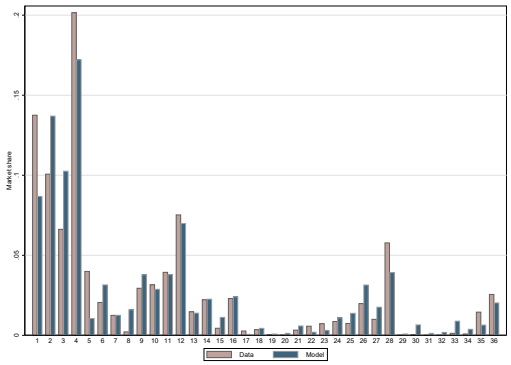
We conduct a number of exercises to assess model fit. Figure E.6 investigates the fit of $F_{c,\kappa\,|\,\mathbf{z}}$ by comparing model-implied choices to the data. Figure E.6a demonstrates very good fit across the dimensions with parameterized mean differences in costs. The fit is reasonable when we look across all thirty-six possible actions (Figure E.6b), considering our parsimonious parameterization of $F_{c,\kappa\,|\,\mathbf{z}}$. The weakest fit of the model is for actions that have relatively low points within their coarsened category, as the model under-predicts these choices relative to the data. We see similar patterns in Figures E.6c and E.6d, which also compare model-implied choices to the data for monetary bids and scores. The fit is very good for the distribution of bids and reasonable for scores. This echoes the patterns in Figure E.6b: we under-predict low scores because we under-predict the share of bidders choosing low-scoring actions. While the fit could be straightforwardly improved by modeling additional mean differences across actions, we view the fit as reasonable for our objectives.

Figure E.6: Model Fit: Costs

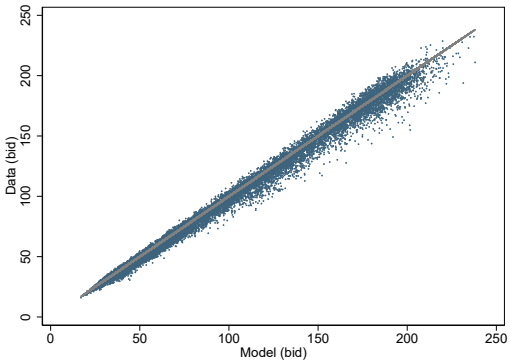
(a) Choice probabilities: coarsened



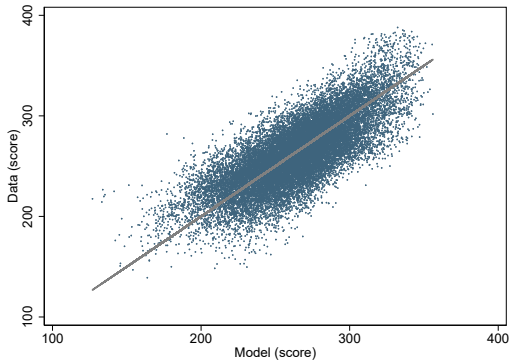
(b) Choice probabilities: all 36 contracts



(c) Bids



(d) Scores



Notes: Figures summarize model fit by comparing simulated choices of contracts, bids, and scores to the data. Panel (a) plots model-implied and observed market shares among the coarsened top-up actions (five dimensions of p_j and the two upgrade dimensions). Panel (b) plots model-implied and observed market shares for all possible contracts. Panels (c) and (d) present scatter plots for the monetary bids (c) and scores (d) comparing model simulations and data. Each dot represents 11 observations (per disclosure requirements).

Table E.3 conducts a second exercise to assess our model-implied costs, comparing them to some administrative (accounting) data collected by the USDA. Because this data is more limited, we aggregate to the three major categories—grasses, trees, and habitats—and compare their relative costs in our model and the data. We estimate the same rank order and generally similar magnitudes. This comparison provides further support that our model fit is reasonable.

Table E.3: Comparison Between Estimated and Administrative Cost Estimates

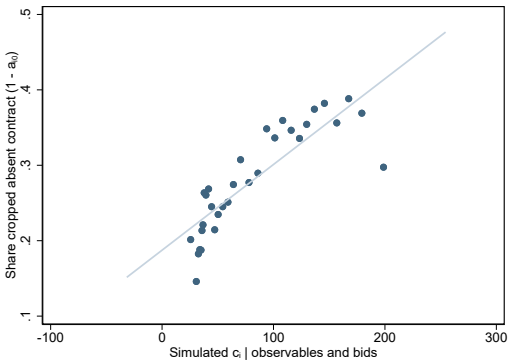
	Estimates (1)	Median admin cost (2)
Tree primary covers (rel. to grasses)	23.77	26.46
Habitat primary covers (rel. to grasses)	15.20	2.67

Notes: Table presents average revealed preference estimates of costs of aggregate primary cover categories, relative to grasses (column 1), compared to administrative data collected on the costs of these actions by the USDA (column 2).

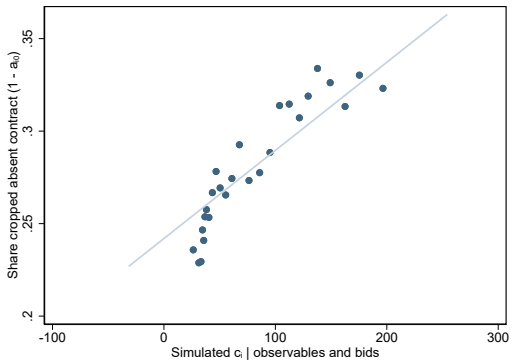
Figures E.7 and E.8 investigate the fit and robustness of our parameterization of $\tau(\mathbf{z}_i, c_i, \kappa_i)$. For each rejected bidder, we can obtain the set of simulation draws for which the observed bid is chosen as optimal. We therefore condition estimates of costs on observables and *the observed bid* and then correlate the base cost with our observations of land use $(1 - a_{i0})$ in Figure E.7. Figure E.7 presents results, both without controls (a) and residualized of observable characteristics (b). Our baseline specification is linear, in order to treat c_i and κ_i symmetrically. But, we also assess robustness to parameterization of $\tau(\mathbf{z}_i, c_i, \kappa_i)$ as a function of $\ln(c)$ in Figure E.8 to investigate deviations from linearity. Results are similar.

Figure E.7: Model Fit: Additionality

(a) Land Use vs. Cost Estimates



(b) Land Use vs. Cost Estimates, Residualized

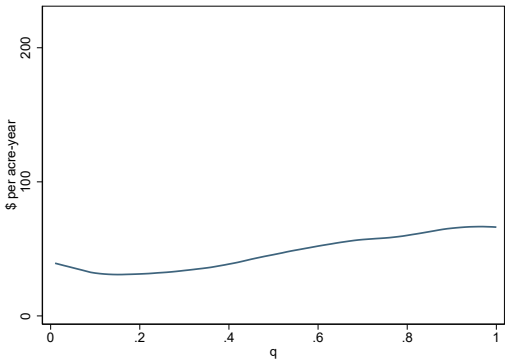


Notes: Figures plot landowner specific additionality for all fields of rejected bidders against the estimate of each bidders' base cost, given parameter estimates $F_{c,\kappa|\mathbf{z}_i}$ and the observed bid. Panel (a) includes no controls (the raw correlation) and panels (b) includes observable controls (it plots the residual correlation).

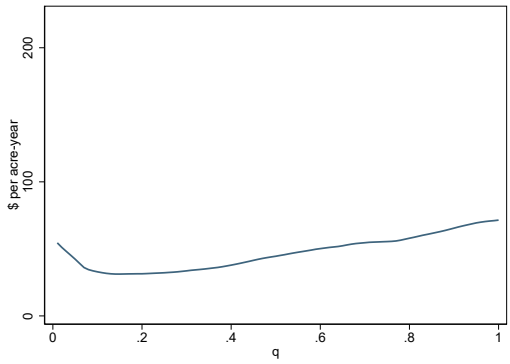
Finally, Figure E.8 investigates robustness to the parameterization and estimation of $\tau(\mathbf{z}_i, c_i, \kappa_i)$ in the context of the empirical graphical analysis. Figure E.8 plots $B \cdot \tau$ curves across the baseline specification (a) and a specification where $\tau(\mathbf{z}_i, c_i, \kappa_i)$ is a function of $\ln(c_i)$ instead of linear in c_i (b). They display similar $B \cdot \tau$ curves—both in their level and slope— indicating similar welfare conclusions across these different parameterizations. Perhaps unsurprisingly, the domain in which they differ most significantly is in extrapolation to the bottom decile of the cost distribution.

Figure E.8: Empirical Graphical Analysis: Robustness to Alternative $B \cdot \tau$

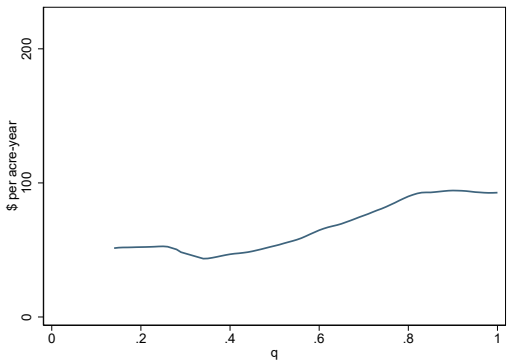
(a) Baseline



(b) Robustness, $\ln(c)$ Parameterization



(c) Robustness, Inversion



Notes: Figure presents robustness of the $B \cdot \tau$ curve in the empirical implementation of the graphical analysis, which denotes the incremental value of contracting, relative to no contract, at each quantile of the population distribution of costs, graphed with local polynomial regressions. The horizontal axis is the share of the population, ordered by costs of accepting a CRP contract. In panels (a)-(b), landowners are ordered by the cost of the base contract. In panel (c) landowners are ordered by the cost of their chosen contract in the CRP auction mechanism. Values are reported in dollars per acre per year. Panel (a) presents our baseline parameterization of $\tau(\mathbf{z}_i, c_i, \kappa_i)$. Panel (b) presents an alternative parameterization of $\tau(\mathbf{z}_i, c_i, \kappa_i) = \pi \cdot \mathbf{z}_i + \beta \cdot \ln(c_i) + \alpha \cdot \kappa_i$. Panel (c) presents $B \cdot \tau$ by plotting the conditional expectation function of observed $B_j(\mathbf{z}_i^s)(1 - a_{i0})$ among landowners at each quantile of $\tilde{c}_i$ defined by equation (22).

Figure E.8c presents results from a simplified model with an alternative assumption of *exogenous contract choices*. While this model does not accurately capture the CRP auction setting, in which contract choice is perhaps the most important dimension of competition,[56] it is useful to consider as a robustness exercise because we can directly compute:

$$\tilde{c}_i = r_i + \frac{G\left(s\left(\left(r_i, \mathbf{x}_i\right), \mathbf{z}_i^s\right)\right)}{\frac{\partial G\left(s\left(\left(r_i, \mathbf{x}_i\right), \mathbf{z}_i^s\right)\right)}{\partial r_i}} \tag{22}$$

from a bidder's first order condition with respect to their monetary bid, r_i. Note that this exercise

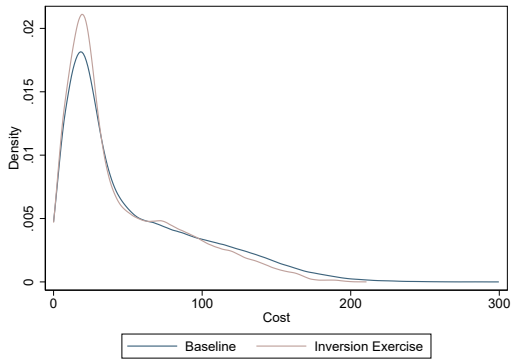
[56]The EBI Factsheets provided to landowners state: "The single most important producer decision involves determining which cover practice to apply to the acres offered. Planting or establishing the highest scoring cover mixture is the best way to improve the chances of offer acceptance."

also assumes away bidcaps and non-linearities in the scoring rule, both of which are relevant and incorporated in our baseline estimation approach. The cost term $\tilde{c}_i$ is defined as the cost associated with a bidder's *chosen contract*. Even without the assumption of exogenous contract choice, we can first compare $\tilde{c}_i$ to our estimated costs of the chosen contract in the status quo mechanism, under our baseline parameterization (Figure E.9).

However, because $\tilde{c}_i$ is defined as the cost associated with a bidder's *chosen contract*, we caution this cost is only interpretable in the graphical welfare analysis under the assumption that contract choice is exogenous. Despite these shortcomings, equation (22) provides the opportunity to examine how additionality varies with costs without parametric assumptions on $\tau(\mathbf{z}_i, c_i, \kappa_i)$. This is because as we have an observation of $\tilde{c}_i$ and additionality (land use) for *each rejected bidder*. Figure E.8c therefore plots expected additionality by the population quantile of $\tilde{c}_i$.

Note that because of the observables in the scoring rule $\mathbf{z}_i^s$ and the choice of contract (here assumed exogenous), bidders with very low monetary bids and (inferred) costs could still be rejected. This would be the case for a bidder with both observables and a contract associated with low point values. However, these rejected low-cost bidders are selected on dimensions that we do not assume are exogenous in our baseline specification. Therefore, to highlight the domain in which we rely on parametric extrapolation in our baseline approach, we exclude quantiles of bidders where the majority are above the winning score threshold and therefore have no observation of $1-a_{i0}$ in Figure E.8c. Similar to the conclusions in panels (a) and (b), the lowest quantiles of the cost distribution is where we are reliant on parametric extrapolation. However, Figure E.8c demonstrates that the shape of the $B \cdot \tau$ curve appears similar to baseline, providing further support that our conclusions are not being driven by our specific parameterization. Note that the level of $B \cdot \tau$ is slightly higher in (c) than in (a)-(b): this is because (c) conditions on the chosen contract, which has higher environmental value than the base contract (plotted in (a)-(b)).

Figure E.9: Estimated Costs at the Chosen Contract



Notes: Figure presents a kernel density plot of estimates of the costs of the chosen CRP contract using our baseline parameterization and estimation approach (described in IV.) and the inversion exercise described above (equation (22)). Our baseline approach conditions on the chosen contract in the simulation, while the alternative approach conditions on the observed chosen contract. Figure restricts to estimates with positive costs.

F Valuing Benefits

We assume that the weights in the scoring rule $B_j(\mathbf{z}_i^s)$ reflect the relative social benefits (in dollars) across j and $\mathbf{z}_i^s$ under the assumption that $a_{i0} = 0$ for all i. The mechanism implicitly makes trade-offs in the scoring rule that monetize relative preferences across contracts and characteristics.

Using this logic requires two assumptions. First, we require the assumption that the scoring rule is indeed constructed under the assumption that $a_{i0} = 0$ for all i. This is motivated directly by a statement from a USDA report (Claassen et al., 2014), which writes: *Benefit-cost indices are used to rank applications for acceptance in all major USDA conservation programs... Existing indices, however, implicitly assume full additionality.* Second, we require that the weights in the scoring rule are not distorted to reduce expenditures. There is no evidence to support this (see Ribaudo et al. (2001) for a discussion of the scoring rule), and the USDA values transfers to agricultural landowners (as revealed by its other programs). We therefore assume that the USDA maximizes social welfare by announcing its preferences in the scoring rule. Of course, the USDA revealed-preferred values of $B_j(\mathbf{z}_i^s)$ may not necessarily align with the true environmental benefits for a variety of reasons, e.g. political concerns. We choose to take this USDA-revealed-preferred approach, versus calibrating $B_j(\mathbf{z}_i^s)$ from an external source, to focus on additionality as a source of social welfare loss.

To calculate these scoring-rule implied relative valuations, we note that scoring rule is separable in the actions incentivized by the heterogeneous contracts and the bid ($) rental rate

$$s(\mathbf{b}_i, \mathbf{z}_i^s) = \underbrace{s_a(\mathbf{x}_i, \mathbf{z}_i^s)}_{\text{action points}} + \underbrace{s_r(r_i)}_{\text{bid rental rate points}} \tag{23}$$

and construct a quasi-linear approximation to the scoring rule to obtain relative willingness to pay. The scoring rule departs from quasi-linearity because of kinked incentives in points bidders receive as a percentage of their bidcap. We "quasi-linearize" the scoring rule by taking the average of $s_r'(r_i)$ in the region without the added percentage points bonus and the region with the percentage point bonus (at the median bidcap value).[57]

Based on this procedure, we obtain estimates of how the USDA trades off higher costs with heterogeneous environmental benefits across contracts j and observable characteristics $\mathbf{z}_i^s$. However, the scoring rule is not directly informative about the level of social benefits. We obtain this using estimates of the value of the CRP from the literature. We assume that all impacts of the CRP accrue only over the contract period. We use following values of the CRP from the literature, where our baseline estimates take the average across these three studies.

1. Our first estimate sums the recreational,[58] public works,[59] and air quality benefits[60] from

[57] The fact that different bidders face different scoring rules based on their bidcap does not reflect differential valuation of environmental benefits across bidders.

[58] This includes sport-fishing, small-game hunting, noncompetitive viewing, and waterfowl hunting.

[59] This includes cost savings associated with reduced maintenance of roadside ditches, navigation channels, water treatment facilities, municipal water uses, flood damage, and water storage.

[60] This includes reduced health risks and cleaning costs associated with blowing dust.

Feather et al. (1999) and adds estimates of the value of greenhouse gas reductions from sequestered CO_2 (over the 10-year contract) and reduced fuel and fertilizer use[61] monetized at \$43 per metric ton. This leads to an overall estimated value of the CRP of \$98.34 per acre, per year. This is likely to be an under-estimate because biodiversity is only valued insofar as it provides recreational benefits, and this estimate does not include water quality improvements from reduced run-off.

2. Our second estimate takes the valuation of the CRP from Hansen (2007), and adds estimates of the value of greenhouse gas reductions from sequestered CO_2 (over the 10-year contract) and reduced fuel and fertilizer use, which then equals \$255.70, per acre, per year.

3. Our third takes the average of a conservative and generous value of the non-GHG CRP benefits from Johnson et al. (2016) and adds estimates of the value of greenhouse gas reductions from sequestered CO_2 (over the 10-year contract) and reduced fuel and fertilizer use. This leads to estimates of \$367.96 and \$456.04, per acre, per year. These may be an over-estimate because benefits are estimated in only one geographic area, which may have more environmentally sensitive land. We average these two effects.

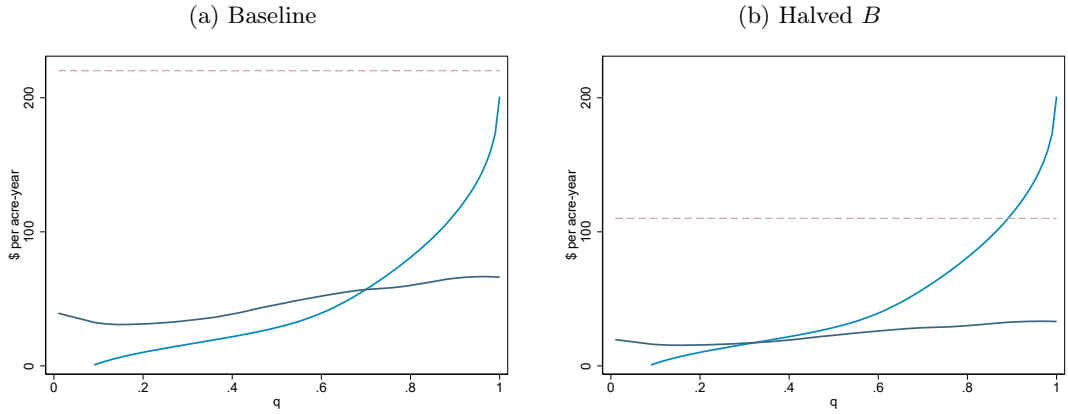
The description above highlights the difficulties of monetizing the value of the all of the environmental benefits of the CRP. We emphasize that our focus is not on obtaining estimates of $B_j(\mathbf{z}_i^s)$, but rather on $\tau(\mathbf{z}_i, c_i, \kappa_i)$; results can be recalculated for any alternative valuation of $B_j(\mathbf{z}_i^s)$. Different estimates of $B_j(\mathbf{z}_i^s)$ will change quantitative conclusions about the social value of the CRP and alternative auctions. However, the main qualitative conclusions persist.

G Supplemental Material: Counterfactuals

Graphical Analysis Appendix Figures G.1 and G.2 assess robustness of the graphical analysis. First, Figure G.1 replicates Figure 7 with valuations of environmental benefits that are halved relative to our baseline estimates (see the discussion above). There still exist social welfare gains, and adverse selection is still apparent. However, with lower valuations of environmental benefits the socially optimal incentives and market size are smaller, with smaller corresponding social welfare gains.

[61] See `https://www.fsa.usda.gov/Assets/USDA-FSA-Public/usdafiles/EPAS/natural-resouces-analysis/nra-landing-index/2017-files/Environmental_Benefits_of_the_US_CRP_2017_draft.pdf`.

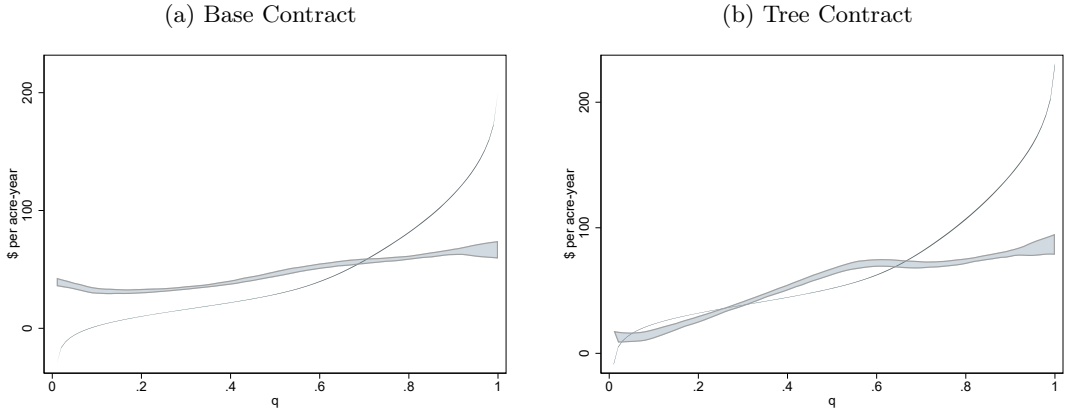
Figure G.1: Graphical Welfare Analysis: Robustness, Lower B



Notes: Figure presents the empirical version of Figure 1 for the base contract, replicating the baseline empirical graphical analysis (Figure 7, re-produced in panel (a)), and an alternative specification with environmental benefits halved relative to baseline (panel (b)). The horizontal axis is the share of the population, ordered by costs of accepting a base CRP contract. Values are reported in dollars per acre per year. The MC curve is the inverse distribution function of the minimum cost to fulfill the base contract. $B \cdot \tau$ denotes the incremental value of contracting, relative to no contract, averaged at each quantile of the population distribution of the base cost, graphed with a local polynomial regression. The vertical distance between the $B \cdot \tau$ and MC curves represents the social surplus from contracting at each quantile of the population distribution of costs. The upwards-sloping $B \cdot \tau$ curve illustrates the presence of adverse selection in the market.

Second, Figure G.2 assesses the robustness of the conclusions in the empirical graphical analysis to estimation error. We do so with the following bootstrap procedure. We (1) re-sample from the population of bidders. Then, for this sample, we (2) estimate parameters with the procedure described in Section IV. and (3) simulate (c_i, κ_i) and $\tau(\mathbf{z}_i, c_i, \kappa_i)$. For each of these simulations, we then (4) re-create the graphical analysis in Figures 7 and 8a. Shaded outcomes represent the range between the 2nd and 98th percentile of 100 iterations of this procedure.

Figure G.2: Empirical Graphical Analysis: Estimation Error



Notes: Figure presents the empirical version of Figure 1 for the base contract (a) and tree-planting and maintenance contracts (b). Shaded lines indicate the range between the 2nd and 98th percentile of bootstrap draws of the procedure described in the text. The horizontal axis is the share of the population, ordered by costs of accepting a CRP contract. Values are reported in dollars per acre per year. The MC curve is the inverse distribution function of the minimum cost to fulfill the contract. $B \cdot \tau$ denotes the incremental value of contracting, relative to no contract, averaged at each quantile of the population distribution of costs, graphed with local polynomial regressions. The vertical distance between the $B \cdot \tau$ and MC curves represents the social surplus from contracting at each quantile of the population distribution of costs. The upwards-sloping $B \cdot \tau$ curve illustrates the presence of adverse selection in the market.

Vickrey Auctions with Scoring Vickrey auctions with scoring maximize a definition of social welfare implied by the scoring rule $s_j(\mathbf{z}_i)$ (equation (18)) subject to two constraints. First, each landowner must obtain at most one contract $\sum_j x_{ij} \leq 1$. Second, no more landowners are allocated contracts, in each auction, than in the status quo. The VCG incentive payment that implements this allocation is:

$$\sum_j s_j(\mathbf{z}_i) \cdot x^*_{ij} + \sum_{i' \neq i} \sum_{j'} \left(s_{j'}(\mathbf{z}_{i'}) - c_{i'} - \kappa_{i'j'} \right) \cdot x^*_{i'j'} - \sum_{i' \neq i} \sum_{j'} \left(s_{j'}(\mathbf{z}_{i'}) - c_{i'} - \kappa_{i'j'} \right) \cdot x^{-i}_{i'j'}, \tag{24}$$

where $\{x^*_{ij}\}$ denotes the allocation that maximizes $\sum_{i'} \sum_{j'} \left(s_{j'}(\mathbf{z}_{i'}) - c_{i'} - \kappa_{i'j'} \right)$ given all reports of $(c_{i'}, \kappa_{i'j'})$ in the population and $\{x^{-i}_{i'j'}\}$ denotes the allocation that solves $\max_x \sum_{i' \neq i} \sum_{j'} \left(s_{j'}(\mathbf{z}_{i'}) - c_{i'} - \kappa_{i'j'} \right) \cdot x^{-i}_{i'j'}$.

Under this incentive payment, bidder i's payoff for contract j is

$$\begin{aligned} \sum_j \left(s_j(\mathbf{z}_i) - c_i - \kappa_{ij} \right) \cdot x^*_{ij} + \sum_{i' \neq i} \sum_{j'} \left(s_{j'}(\mathbf{z}_{i'}) - c_{i'} - \kappa_{i'j'} \right) \cdot x^*_{i'j'} \\ - \sum_{i' \neq i} \sum_{j'} \left(s_{j'}(\mathbf{z}_{i'}) - c_{i'} - \kappa_{i'j'} \right) \cdot x^{-i}_{i'j'}, \end{aligned} \tag{25}$$

such that equations (18) and (25) are equivalent from the perspective of bidder i's report. Bidders therefore truthfully report their vector of (c_i, κ_i), then are ranked by $\max_j s_j(\mathbf{z}_i) - c_i - \kappa_{ij}$. The highest scoring bidders subject to the auction's quantity constraint are allocated the contract

$\arg\max_j s_j(\mathbf{z}_i) - c_i - \kappa_{ij}$.

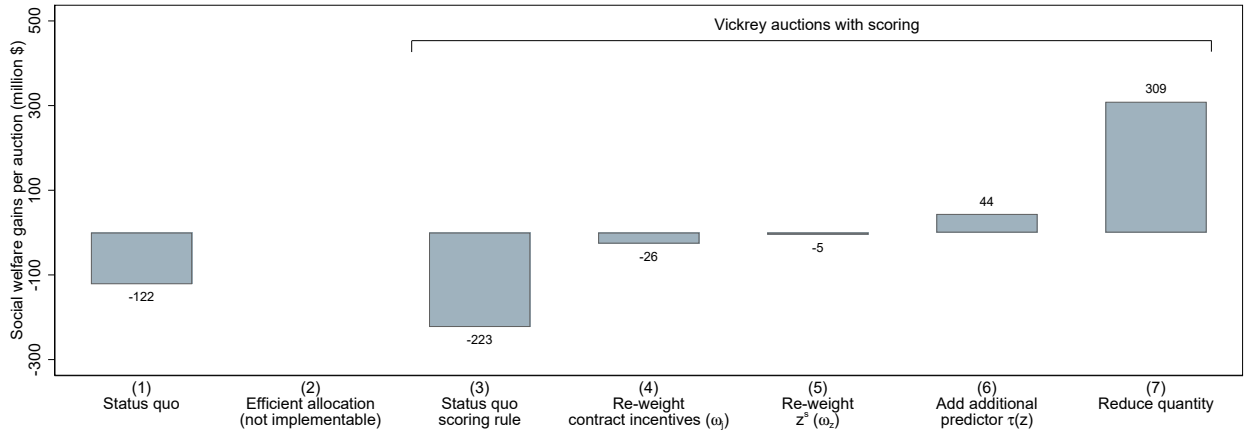
Other Alternative Auctions A key advantage of the Vickrey auctions with scoring is that the equilibrium allocations are simple to compute. However, it is useful to know how the alternative scoring rule would impact allocations under the status quo auction format, where each bidder solves equation (10). To implement this counterfactual, we assume that bidders' beliefs about the acreage limit and the number of competing bidders is held fixed. However, we allow beliefs about the equilibrium distribution of scores to adjust using the following procedure:

1. Initialize an empirical distribution of scores. We begin with optimal bids, scored under the new scoring rule, given beliefs based on the status quo distribution of scores.
2. Solve the inner problem (see equation (11)), for all possible integer scores.
3. Iterate the following (for each step k):
   (a) Resample from step $k-1$'s distribution of bidders' scores in the procedure described in Step 1 of Appendix Section E. Estimate a kernel density of the resulting distribution of threshold scores using a Gaussian kernel and a bandwidth of 5, as in baseline ($G^k(S)$).
   (b) Solve for step k scores: solve for each bidder's optimal score, given the inner problem (solved in Step 2), the scoring rule, and beliefs from (a), $G^k(S)$ (see equation (12)),
   (c) Compare the difference between the estimated CDF at each score S in step k and $k-1$. Repeat until the max absolute value of the difference (across integer scores) falls below a critical threshold.

We conduct this procedure for each auction. We hold fixed the draws of acreage limits, number of competing bidders, and bootstrap draws of bidders across iterations; for some auctions, we required a dampening parameter to achieve convergence. We then use these beliefs to calculate optimal bids and allocations, given the alternative scoring rule, reported in column (9) of Table 5.

Cost of Public Funds Figure G.3 considers the same auctions presented in Figure 9, but evaluates social welfare with a cost of funds equal to 0.15. Under this framework, 15% of all USDA spending is considered deadweight loss, motivated by the social costs of financing expenditures via distortionary taxation. With a cost of funds, the status quo auction reduces social welfare. However, social welfare gains become positive once the auction is designed to consider additionality. Note that Figure G.3 evaluates auctions using the same scoring rules as in Figure 9. With weights ω_j and $\omega_{\mathbf{z}}$ re-optimized to reduce government spending, gains would be higher.

Figure G.3: Social Welfare Under Alternative Auctions: Cost of Funds



Notes: Figure presents estimates of the social welfare gains (defined in equation (16), with the addition of a cost of funds equal to 0.15) under status quo and alternative auctions. Results reported in million dollars per auction. All auctions impose that each landowner obtains at most one contract and that total contracts awarded cannot exceed the status quo, in each auction. Bar (1) simulates the status quo. Bar (2) is excluded because USDA spending is undefined. Bars (3)-(7) calculate social welfare under alternative Vickrey auctions with scoring (see Section V. for more details). Bars (3)-(6) hold quantity (the number of landowners allocated contracts, in each auction) constant at the status quo and change the scoring rule $s_j(\mathbf{z}_i)$ defined in equation (17). Bar (3) uses the existing scoring rule $s_j(\mathbf{z}_i) = B_j(\mathbf{z}_i^s)$. Bar (4) uses a scoring rule with the social-surplus maximizing incentives across contracts (ω_j) (with social surplus defined in equation (16)). Bar (5) uses a scoring rule with the social-surplus maximizing asymmetry terms across bidders using characteristics already in the scoring rule ($\mathbf{z}_i^s$). Bar (6) adds an additional characteristic to the scoring rule, a prediction of $\tau(\mathbf{z}_i, c_i, \kappa_i)$ based on immutable characteristics of landowners already collected by the USDA (deciles of soil productivity and wind and water erosion). Bar (7) uses the same scoring rule as bar (6) but reduces the number of contracts allocated to landowners: only landowners with positive scoring-rule-implied social surplus $\max_j s_j(\mathbf{z}_i) - c_i - \kappa_{ij} \geq 0$ are awarded contracts. The allocations are the same as in Figure 9, but are evaluated under an objective that incorporates a cost of funds equal to 0.15.

Posted Prices Mechanisms Instead of administering a scoring auction, the USDA could post prices. Prices that vary across observables and the menu of contracts, $t_j(\mathbf{z}_i) = \omega_{\mathbf{z}} \cdot \mathbf{z}_i + \omega_j$, achieve the same objective as the scoring rule, $s_j(\mathbf{z}_i)$. While posted prices do not meet the quantity constraint exactly, they are simple, used by the USDA (e.g. in Continuous CRP), and can also be constructed to satisfy a range of objectives that balance both efficiency and expenditures. Table G.1 illustrates. Columns (1) and (2) serve as benchmarks, and Columns (3)-(5) construct incentives $t_j(\mathbf{z}_i)$ to maximize objectives that — in contrast to our baseline counterfactuals in Table 5 — explicitly consider USDA spending.

Table G.1: Posted Prices Mechanisms

	$t_j(\mathbf{z}_i)$ to maximize:				
	Status quo auction	Social surplus (no quantity constraint)	Social surplus with a cost of public funds	Environmental value net of expenditures	Dominating $t_j(\mathbf{z}_i)$
	(1)	(2)	(3)	(4)	(5)
Social welfare	120	485	460	350	403
USDA spending	1,615	985	583	219	1,556
Landowner surplus	666	588	336	136	853
Environmental value	1,069	882	707	434	1,105
Share awarded contract	0.81	0.67	0.55	0.33	0.81

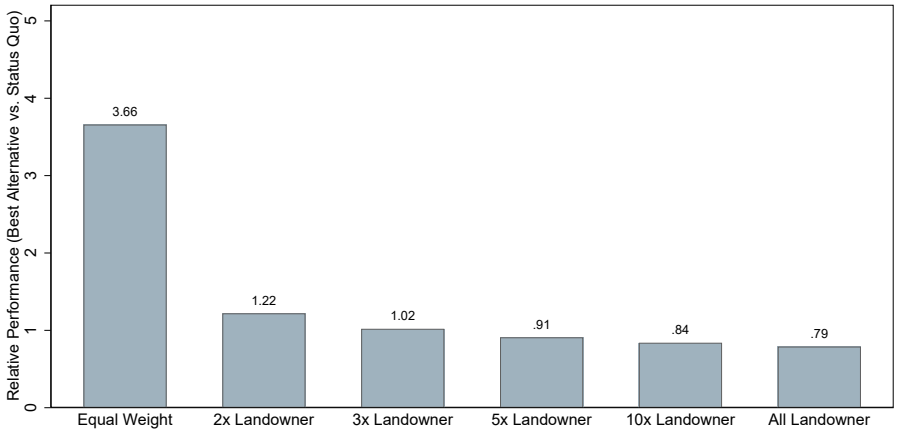
Notes: Table presents results under current and alternative posted prices mechanisms. It tabulates social welfare (equation (16)), USDA spending, landowner surplus, and environmental value $\sum_i \sum_j B_j\left(\mathbf{z}_i^s\right) \cdot \tau\left(\mathbf{z}_i, c_i, \kappa_i\right) \cdot x_{ij}$ in million dollars per auction, and the share of landowners with a contract. Each landowner obtains at most one contract. Column (1) simulates the status quo. Column (2) uses social-surplus maximizing incentives across contracts, characteristics already in the scoring rule ($\mathbf{z}_i^s$), and the additionality factor. Columns (3)-(5) use the same observables as column (2) and vary the weights $\omega_{\mathbf{z}}$ and ω_j. Column (3) calculates $t_j(\mathbf{z}_i)$ to maximize $\sum_i \sum_j \left(B_j\left(\mathbf{z}_i^s\right) \cdot \tau\left(\mathbf{z}_i, c_i, \kappa_i\right) - c_i - \kappa_{ij} - 0.15 \cdot t_j(\mathbf{z}_i)\right) \cdot x_{ij}$, and column (4) calculates $t_j(\mathbf{z}_i)$ to maximize $\sum_i \sum_j \left(B_j\left(\mathbf{z}_i^s\right) \cdot \tau\left(\mathbf{z}_i, c_i, \kappa_i\right) - t_j(\mathbf{z}_i)\right) \cdot x_{ij}$. Column (5) calculates $t_j(\mathbf{z}_i)$ to implement an allocation with higher social welfare, landowner surplus, and environmental value, and lower USDA spending, holding the quantity constant on average across auctions.

Alternative Objectives Our baseline assumption evaluates social welfare based on equation (16). We explore the possibility that the USDA may place higher weight on landowner surplus than environmental services procured (net of spending), and whether this could rationalize the performance of the status quo auction. We consider the following objective:

$$\sum_i \sum_j \left(\frac{2}{1+\lambda} \cdot \left(B_j\left(\mathbf{z}_i^s\right) \cdot \tau\left(\mathbf{z}_i, c_i, \kappa_i\right) - r_{ij}\right) + \frac{2\lambda}{1+\lambda} \cdot \left(r_{ij} - c_i - \kappa_{ij}\right) \right) \cdot x_{ij}, \tag{26}$$

where r_{ij} is the transfer from the USDA to the landowner and λ parameterizes the relative weight on landowner surplus versus environmental services procured net of costs. For $\lambda = 1$, equation (26) is equivalent to equation (16). In Figure G.4, we report the relative performance of the highest performing auction (bar (7) in Figure 9) relative to the status quo (bar (1) in Figure 9), evaluated based on equation (26) as we vary the weights $\lambda = \{1, 2, 10, \infty\}$.

Figure G.4: Evaluating Alternative vs. Status Quo Auctions under Alternative Objectives



Notes: Figure reports the ratio of the objective in equation (26) evaluated at the allocation under the best performing auction (bar (7) in Figure 9 versus the status quo (bar (1)) in Figure 9), for varying weights $\lambda = \{1, 2, 10, \infty\}$.

Limited Information Scoring Rule We assume that the function $\tau(\mathbf{z}_i, c_i, \kappa_i)$ is stable across time. Our baseline alternative scoring rule also requires knowledge of both the distribution $F_{c,\kappa \mid \mathbf{z}}$ and the function $\tau(\mathbf{z}_i, c_i, \kappa_i)$ to construct. This assumption and demanding information requirements could limit the use of the alternative scoring rules prospectively.

We therefore construct an alternative scoring rule that requires no knowledge of the distribution of $F_{c,\kappa \mid \mathbf{z}}$ (or our estimated $\tau(\mathbf{z}_i, c_i, \kappa_i)$) to construct. We can evaluate this scoring rule out-of-sample to assess our assumption about the stability of $\tau(\mathbf{z}_i, c_i, \kappa_i)$. As an additional benefit, it is also a far simpler procedure than our baseline approach and could reasonably be implemented by a program administrator. We estimate the rule as follows, pooling past auctions:

1. Estimate tract-level regressions of cropping rates on observables $\mathbf{z}_i$ in the year of the auction, prior to the contract (see estimates in Figure D.7). We use as observables the same 32 cells of prior land use, prior CRP status, and soil productivity as in our baseline parameterization. Call the fitted values from this regression $\tilde{\tau}(\mathbf{z}_i)$.

2. Collect the RD point estimates of additionality across past auctions $\hat{\beta}_g^a$ (see estimates in Table D.2). Define $\tau(\mathbf{z}_i) = \tilde{\tau}(\mathbf{z}_i) + \upsilon$ and estimate υ to match the RD additionality estimates, such that
$$\mathbb{E}\left[\tau(\mathbf{z}_i) - \hat{\beta}_g^a \mid \underline{S}_g - b < s(\mathbf{b}_i^*, \mathbf{z}_i^s) =< \underline{S}_g + b\right] = 0$$
for bandwidth b, with equal weight to each past auction.

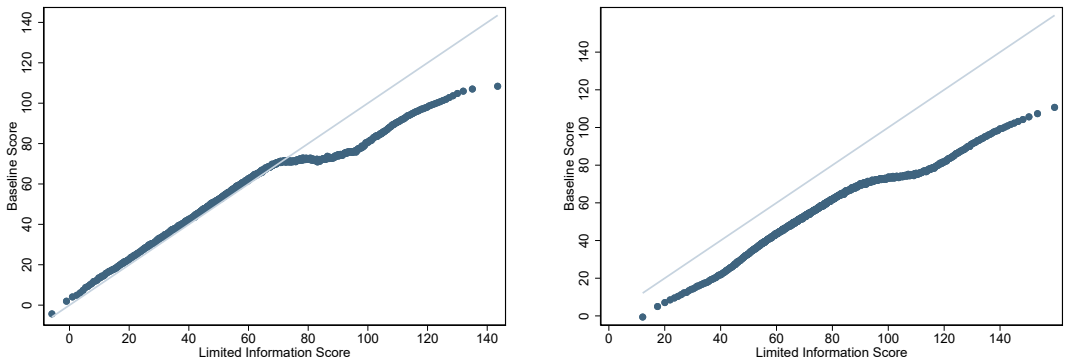
3. Project onto characteristics used in the scoring rule. Regress $B_j(\mathbf{z}_i^s) \cdot \tau(\mathbf{z}_i)$ on the immutable characteristics used in the scoring rule and across contracts, obtaining different coefficients on the same observables as in our baseline approach (see equation (17)). We will refer to this scoring rule as the limited information scoring rule.

This approach uses only the raw data available to the USDA — matched bids and land use — without requiring estimates of costs or the ability to observe a large share of losers and delineations of their bid fields as in the 2016 auction and our baseline approach.

We construct the scoring rule using auctions pre-2016, and evaluate its performance on the held-out 2016 auction. 2016 is a useful year for testing because our estimates of $\tau(\mathbf{z}_i, c_i, \kappa_i)$ leverage data from only this most-restrictive auction. Figure G.5 presents binned scatterplots of the baseline preferred scoring rule and this alternative limited information scoring rule, estimated in the same remote-sensing data as in baseline estimation (a) and in the administrative data (b). While they do not match exactly, the two scoring rules are highly correlated. Unsurprisingly, using different datasets leads to a greater difference between the limited information and baseline rules. In particular, scoring rules constructed in the administrative data are higher on average, consistent with the larger regression discontinuity results of additionality in the administrative data (compare Table 2 column (2) versus column (1)).

Figure G.5: Baseline vs. Limited Info Scoring Rule

(a) Constructed using Remote-Sensing Data (Same) (b) Constructed using Admin Data (Different)



Notes: Figure presents binned scatterplots of the baseline highest performing scoring rule (used in column (6) of Table 5) versus the limited information scoring rule described in this section, across bidders, contracts, and auctions. Panel (a) presents the limited information scoring rule estimated in the remote sensing data. Panel (b) presents the limited information scoring rule estimated in the administrative data (used in column (10) of Table 5).

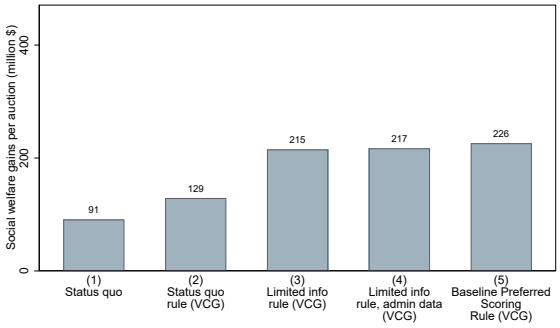
Figure G.6 presents results. Figure G.6a evaluates the limited information scoring rule in the 2016 hold-out auction. We present social welfare gains — all evaluated using equation (16) and our estimates of $F_{c,\kappa \mid \mathbf{z}}$ and $\tau(\mathbf{z}_i, c_i, \kappa_i)$ — under the status quo auction (bar (1)), the Vickrey auction with scoring with the baseline rule (bar (2)), and the Vickrey auction with scoring with the limited information rule (bar (3)). We also use this approach to evaluate the sensitivity of our results to our choice of dataset by constructing the limited information scoring rule using the administrative data (bar (4)). We benchmark the performance gains against our baseline preferred scoring rule (bar (5)). We find that even this simple procedure to adjust the scoring rule yields substantial social welfare gains. Figure G.6b presents a similar conclusion, across all auctions.[62]

[62]The total quantity procured is constant across counterfactual auctions in Figure G.6a because the quantity

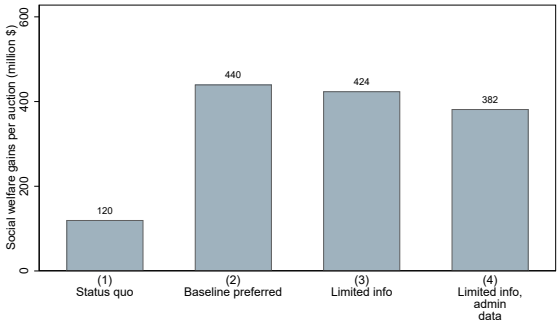
Figure G.6c also illustrates similar socially-optimal market sizes under the baseline preferred and limited information scoring rules in all seven auctions. If we construct the limited information scoring rule using the administrative data, we obtain slightly higher estimates of the socially-optimal market size, consistent with the slightly higher RD estimates of additionality in Section III. However, social welfare gains under the scoring rule constructed in the administrative data, but evaluated in the remote sensing data, are still large (see bar (4) of Figure G.6b).

Figure G.6: Limited Information Scoring Rule: Evaluation

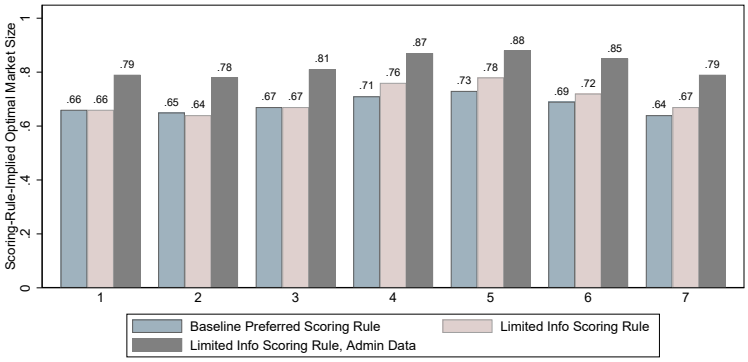
(a) Alternative Auctions, 2016 Evaluation (Hold Out)



(b) Alternative Auctions, All Auctions



(c) Estimated Market Size per Auction: Limited Info vs. Baseline



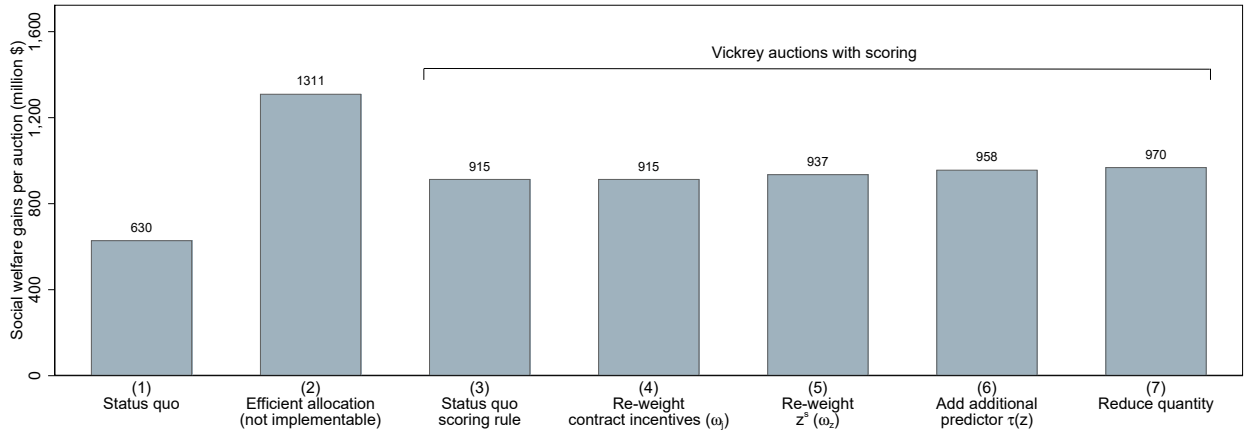
Notes: Figure presents estimates of the social welfare gains (panels (a) and (b)) and socially-optimal market sizes (panel (c)) under alternative auctions. Social welfare is defined in equation (16) and uses estimates of $F_{c,\kappa \mid \mathbf{z}}$ and $\tau(\mathbf{z}_i, c_i, \kappa_i)$; results reported in million dollars per auction. All auctions impose that each landowner obtains at most one contract and that total contracts awarded cannot exceed the status quo. The limited information scoring rule is constructed using only pre-2016 data (described in the appendix text). Panel (a) presents estimates for the 2016 auction only. This is the most restrictive auction used to estimate $\tau(\mathbf{z}_i, c_i, \kappa_i)$, and is held out of the limited information scoring rule construction. Bar (1) simulates the status quo, bar (2) simulates a Vickrey auction with scoring using the status quo rule, bar (3) simulates a Vickrey auction with scoring using the limited information scoring rule estimated with the remote sensing data, bar (4) simulates a Vickrey auction with scoring using the limited information scoring rule estimated with the administrative data, and bar (5) simulates a Vickrey auction with scoring using the highest performing scoring rule in Figure 9. All bars of Panel (a) hold quantity constant at the status quo. Panel (b) presents estimates for all auctions. Bar (1) simulates the status quo and bar (2) simulates a Vickrey auction with scoring using the baseline preferred scoring rule (these replicate bars (1) and (7) of Figure 9). Bars (3) and (4) simulate Vickrey auction with scoring using the limited information scoring rule estimated with the remote sensing data (bar (3)) and administrative data (bar (4)). Panel (c) presents estimates of the socially optimal market size (the share of landowners awarded contracts) under each scoring rule in each of the seven auctions (ordered chronologically).

constraint binds in 2016. In Figure G.6b, the auctions in bars (2)-(4) reject landowners with $\max_j s_j(\mathbf{z}_i) - c_i - \kappa_{ij} < 0$, decreasing quantity procured relative to the status quo (bar (1)).

Top-Up Actions not Affected by Additionality For all analyses beyond those restricted to the base contract, we require an assumption about how additionality impacts the social value derived from the top-up actions that differentiate the contracts in the mechanism. This is due to fundamental data limitations. Our primary specification defines the social benefit of contracting as $B_j\left(\mathbf{z}_i^s\right) \cdot \tau\left(\mathbf{z}_i, c_i, \kappa_i\right)$. In this specification, no social benefits are generated when a landowner is not additional. This could be either because, as with land retirement, top-up actions (or close substitutes) would have occurred even absent a CRP contract. It could also be motivated by an assumption that land retirement and the top-up actions are complements in the USDA's valuation of contracting. We view this assumption as reasonable for many of the important actions being incentivized, e.g. grassland and tree maintenance. For example, as discussed in the main text, we can test this assumption by leveraging the fact that we can distinguish between trees and grasses in the remote sensing data. We find that over 60% of rejected bidders choosing a tree contract have the majority of their bid land in trees, and 92% have some trees on their bid land.

However, in this section, we consider an alternative assumption in which the incremental actions incentivized by the contracts are always additional. Specifically, we consider an alternative valuation of contracts equal to $B_0\left(\mathbf{z}_i^s\right) \cdot \tau\left(\mathbf{z}_i, c_i, \kappa_i\right) + B^j\left(\mathbf{z}_i^s\right)$, where $B_0\left(\mathbf{z}_i^s\right)$ is the social benefit of the base action and $B^j\left(\mathbf{z}_i^s\right)$ is the incremental social benefit of the top-up action beyond the base action. This could be motivated by a scenario in which contracting impacted the specific species mix, which we assume the USDA values at $B^j\left(\mathbf{z}_i^s\right)$, even if it did not impact land retirement. Under this assumption, over one third of the total social surplus at stake is not impacted by additionality at all. This makes correctly incentivizing the top-up actions — whose relative valuations are derived solely from monetizing the scoring rule — matter substantially to the performance of the mechanism.

Figure G.7: Social Welfare Under Alternative Auctions: Alternative Top-Up Assumption



Notes: Figure presents estimates of the social welfare gains (defined in equation (16), but replacing $B_j\left(\mathbf{z}_i^s\right) \cdot \tau\left(\mathbf{z}_i, c_i, \kappa_i\right)$ with $B_0\left(\mathbf{z}_i^s\right) \cdot \tau\left(\mathbf{z}_i, c_i, \kappa_i\right) + B^j\left(\mathbf{z}_i^s\right)$ where $B_0\left(\mathbf{z}_i^s\right)$ is the social benefit of the base action and $B^j\left(\mathbf{z}_i^s\right)$ is the incremental value of the top-up action) under status quo and alternative auctions. Results reported in million dollars per auction. All auctions impose that each landowner obtains at most one contract and that total contracts awarded cannot exceed the status quo, in each auction. Bar (1) simulates the status quo. Bar (2) calculates the social welfare gains under an efficient allocation that allocates contracts using all $\mathbf{z}_i$ and (c_i, κ_i) to maximize equation (16). Due to adverse selection, this allocation may not be implementable. Bars (3)-(7) calculate social welfare under alternative Vickrey auctions with scoring (see Section V. for more details). Bars (3)-(6) hold quantity (the number of landowners allocated contracts, in each auction) constant at the status quo and change the scoring rule $s_j\left(\mathbf{z}_i\right)$ defined in equation (17). Bar (3) uses the existing scoring rule $s_j\left(\mathbf{z}_i\right) = B_j\left(\mathbf{z}_i^s\right)$. Bar (4) uses a scoring rule with the social-surplus maximizing incentives across contracts (ω_j). Bar (5) uses a scoring rule with the social-surplus maximizing asymmetry terms across bidders using characteristics already in the scoring rule $(\mathbf{z}_i^s)$. Bar (6) adds an additional characteristic to the scoring rule, a prediction of $\tau\left(\mathbf{z}_i, c_i, \kappa_i\right)$ based on immutable characteristics of landowners already collected by the USDA (deciles of soil productivity and wind and water erosion). Bar (7) uses the same scoring rule as bar (6) but reduces the number of contracts allocated to landowners: only landowners with positive scoring-rule-implied social surplus $\max_j s_j\left(\mathbf{z}_i\right) - c_i - \kappa_{ij} \geq 0$ are awarded contracts.

Figure G.7 re-creates Figure 9 under this alternative assumption. Social welfare under the status quo is higher, but the status quo still achieves less than half of the social welfare gains under the efficient allocation. The biggest difference between Figures 9 and G.7 is the large social welfare gains from the switch to the VCG mechanism, holding the scoring rule constant (bar (3)). This is because the Vickrey auction with scoring using the status quo rule now efficiently incentivizes choices across contracts. Because the top-up actions represent a large share of social welfare gains at stake in the mechanism, incentivizing them efficiently is important for the auction's performance. Adjusting the mechanism for heterogeneity in additionality is still quantitatively important: moving from bar (3) to bar (6) increases social welfare by 7% of the status quo, or 13% of the gains of the improvement between bar (1) and bar (6). Also as in our baseline estimates, quantity procured is higher than is socially optimal.

We emphasize that the exercise of Figure G.7 is not to document that results are quantitatively the same under this alternative assumption versus our baseline assumption. The assumptions are very different, so naturally lead to some different quantitative implications. Instead, we highlight that the insights from our baseline assumption are quantitatively relevant even when a large share of the surplus at stake in the mechanism $(B^j\left(\mathbf{z}_i^s\right))$ is not impacted by additionality.

References

Ackerberg, Daniel A., "A new use of importance sampling to reduce computational burden in simulation estimation," *QME*, December 2009, *7* (4), 343–376.

Akerlof, George A., "The Market for "Lemons": Quality Uncertainty and the Market Mechanism," *The Quarterly Journal of Economics*, 1970, *84* (3), 488–500.

Alix-Garcia, Jennifer and Daniel Millimet, "Remotely Incorrect? Accounting for Nonclassical Measurement Error in Satellite Data on Deforestation," *Journal of the Association of Environmental and Resource Economists*, December 2022.

Calonico, Sebastian, Matias D. Cattaneo, and Rocio Titiunik, "Robust Nonparametric Confidence Intervals for Regression-Discontinuity Designs," *Econometrica*, 2014, *82* (6), 2295–2326.

Claassen, Roger, Roger Horowitz, Eric Duquette, and Kohei Ueda, "Additionality in U.S. Agricultural Conservation and Regulatory Offset Programs," Technical Report ERR-170, U.S. Department of Agriculture, Economic Research Service July 2014.

Feather, Peter, Daniel Hellerstein, and LeRoy T. Hansen, "Economic Valuation of Environmental Benefits and the Targeting of Conservation Programs: The Case of the CRP," *Agricultural Economic Reports*, 1999.

Hansen, LeRoy, "Conservation Reserve Program: Environmental Benefits Update," *Agricultural and Resource Economics Review*, October 2007, *36* (2), 267–280.

Hortaçsu, Ali, "Mechanism Choice and Strategic Bidding in Divisible Good Auctions: An Empirical Analysis Of the Turkish Treasury Auction Market," November 2000.

_ **and David McAdams**, "Mechanism Choice and Strategic Bidding in Divisible Good Auctions: An Empirical Analysis of the Turkish Treasury Auction Market," *Journal of Political Economy*, October 2010, *118* (5), 833–865.

Johnson, Kris A., Brent J. Dalzell, Marie Donahue, Jesse Gourevitch, Dennis L. Johnson, Greg S. Karlovits, Bonnie Keeler, and Jason T. Smith, "Conservation Reserve Program (CRP) lands provide ecosystem service benefits that exceed land rental payment costs," *Ecosystem Services*, April 2016, *18*, 175–185.

Lark, Tyler J., Richard M. Mueller, David M. Johnson, and Holly K. Gibbs, "Measuring land-use and land-cover change using the U.S. department of agriculture's cropland data layer: Cautions and recommendations," *International Journal of Applied Earth Observation and Geoinformation*, October 2017, *62*, 224–235.

Ribaudo, Marc O., Dana L. Hoag, Mark E. Smith, and Ralph Heimlich, "Environmental indices and the politics of the Conservation Reserve Program," *Ecological Indicators*, August 2001, *1* (1), 11–20.

Torchiana, Adrian L., Ted Rosenbaum, Paul T. Scott, and Eduardo Souza-Rodrigues, "Improving Estimates of Transitions from Satellite Data: A Hidden Markov Model Approach," *The Review of Economics and Statistics*, December 2024, pp. 1–16.